Modeling the magnetic fields in radio galaxies and quasars

Martín Huarte Espinosa
<martinhe@pas.rochester.edu>

In collaboration with Paul Alexander, Martin Krause, Christian Kaiser, Jongsoo Kim, David Titterington and Volker Gaibler.

University of Rochester
Department of Physics and Astronomy
15 October '09

Galaxy Cluster MS 0735.6+7421

CXO ▪ HST ▪ VLA

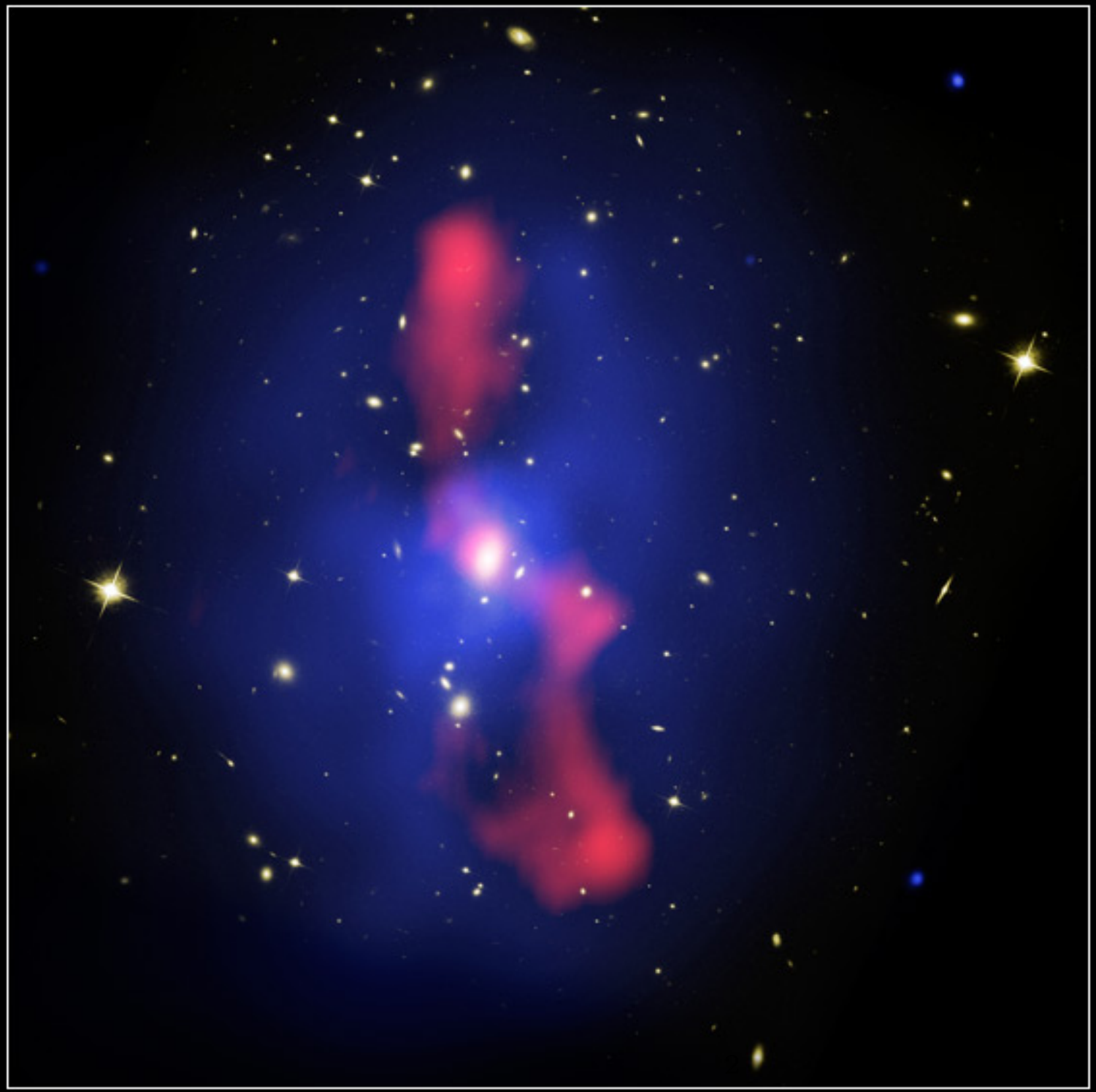

X-ray
Chandra X-Ray Observatory

Visible
Hubble Space Telescope

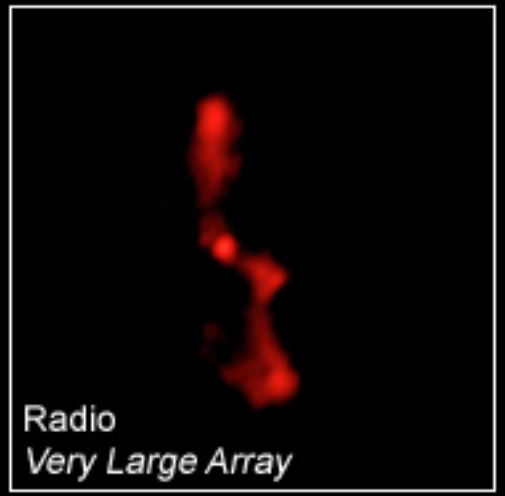

Radio
Very Large Array

NASA, ESA, CXC/NRAO/STScI, B. McNamara (University of Waterloo and Ohio University) STScI-PRC06-51

Extragalactic radio sources

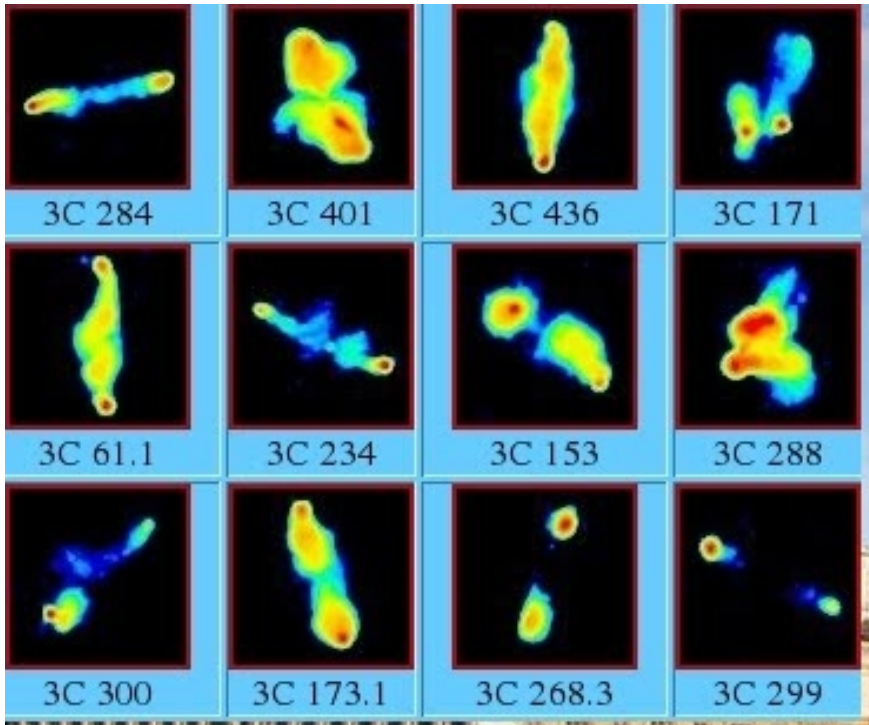

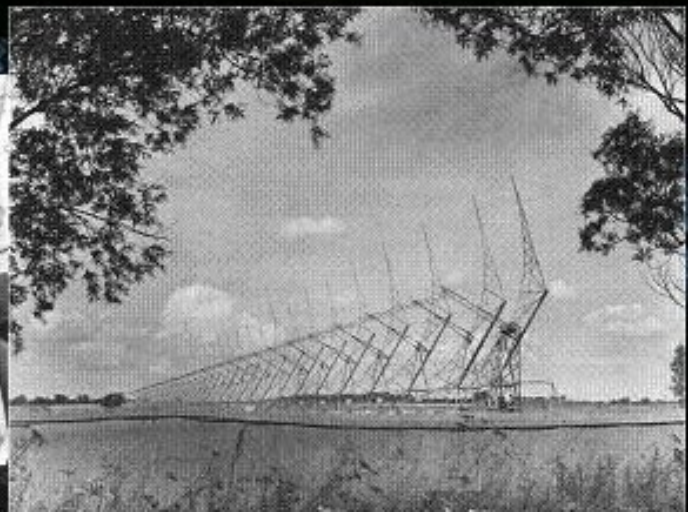

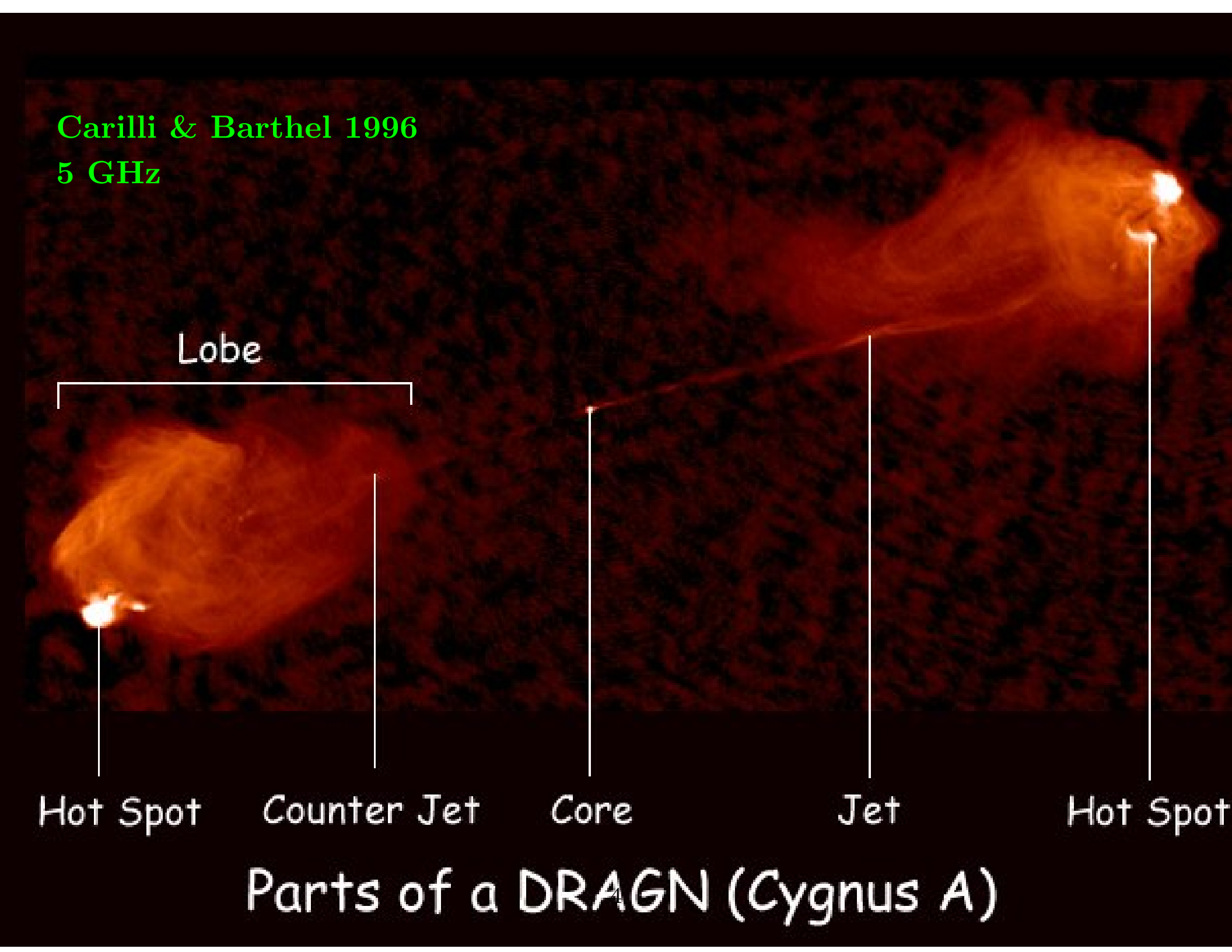
Carilli & Barthel 1996
5 GHz
Lobe
Hot Spot
Counter Jet
Core
Jet
Hot Spot
Parts of a DRAGN (Cygnus A)

Formation and evolution

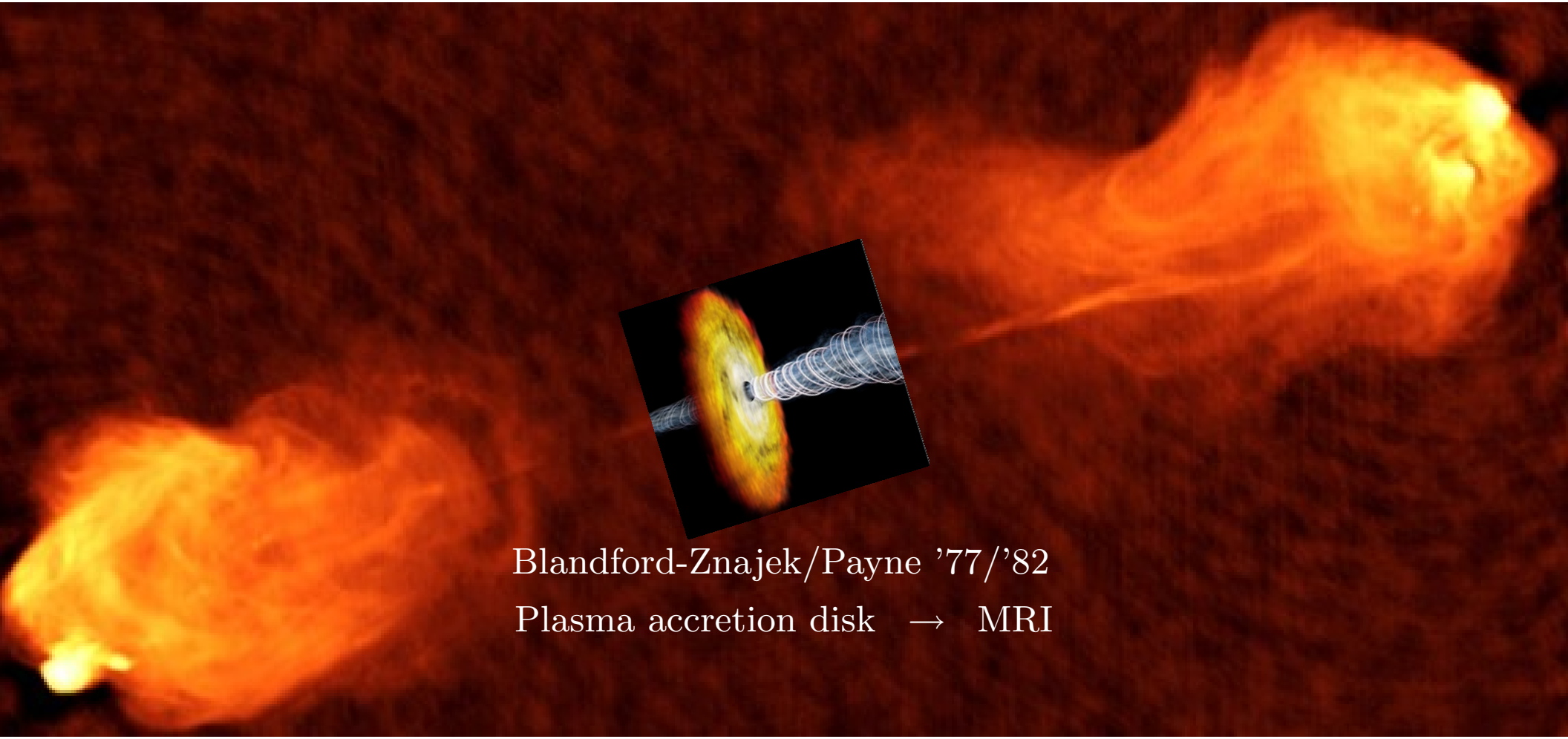

Blandford-Znajek/Payne '77/'82

Plasma accretion disk $\rightarrow$ MRI

Formation and evolution

Sam Falle 1991

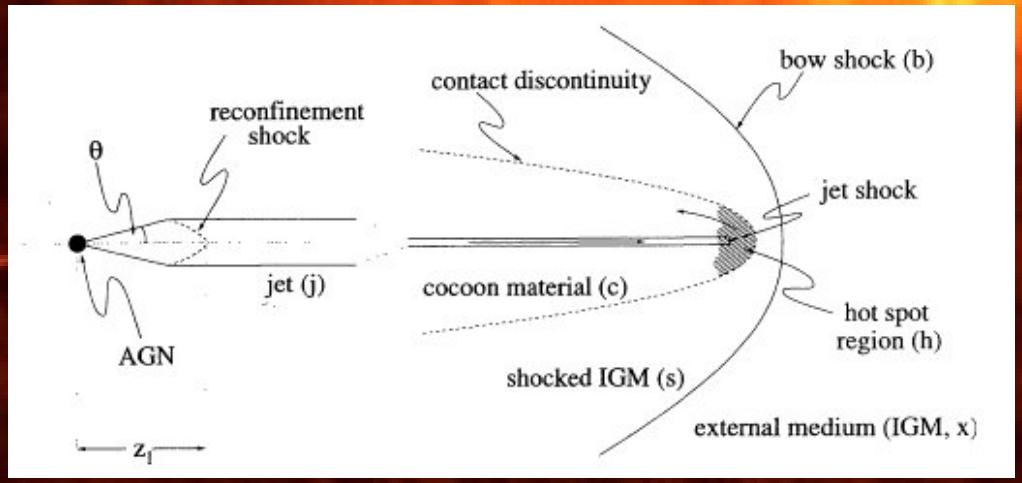

Self-similar model

Kaiser & Alexander '97

The ICM
X-ray Bremsstrahlung

$T \sim 10^8\,\mathbf{K}$
$\rho \sim 10^{-2}\,\mathbf{cm}^{-3}$

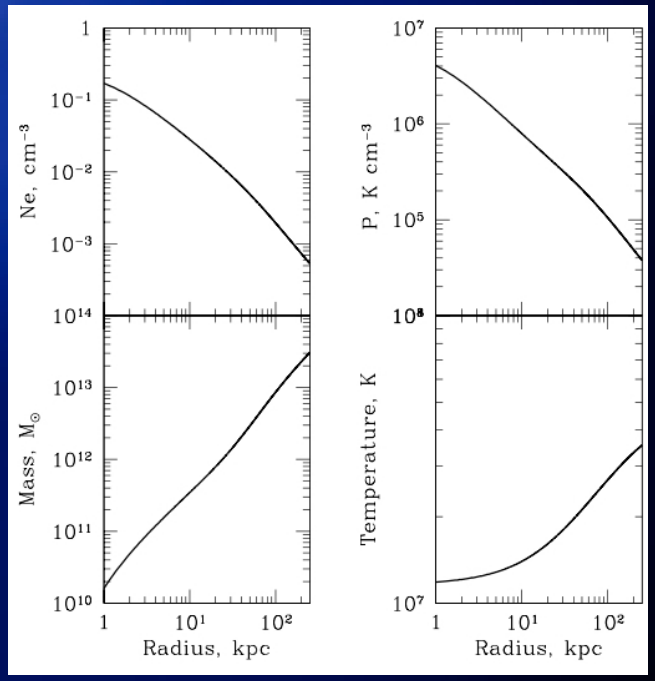

Nulsen & Böhringer 1995

The magnetic fields in galaxy clusters

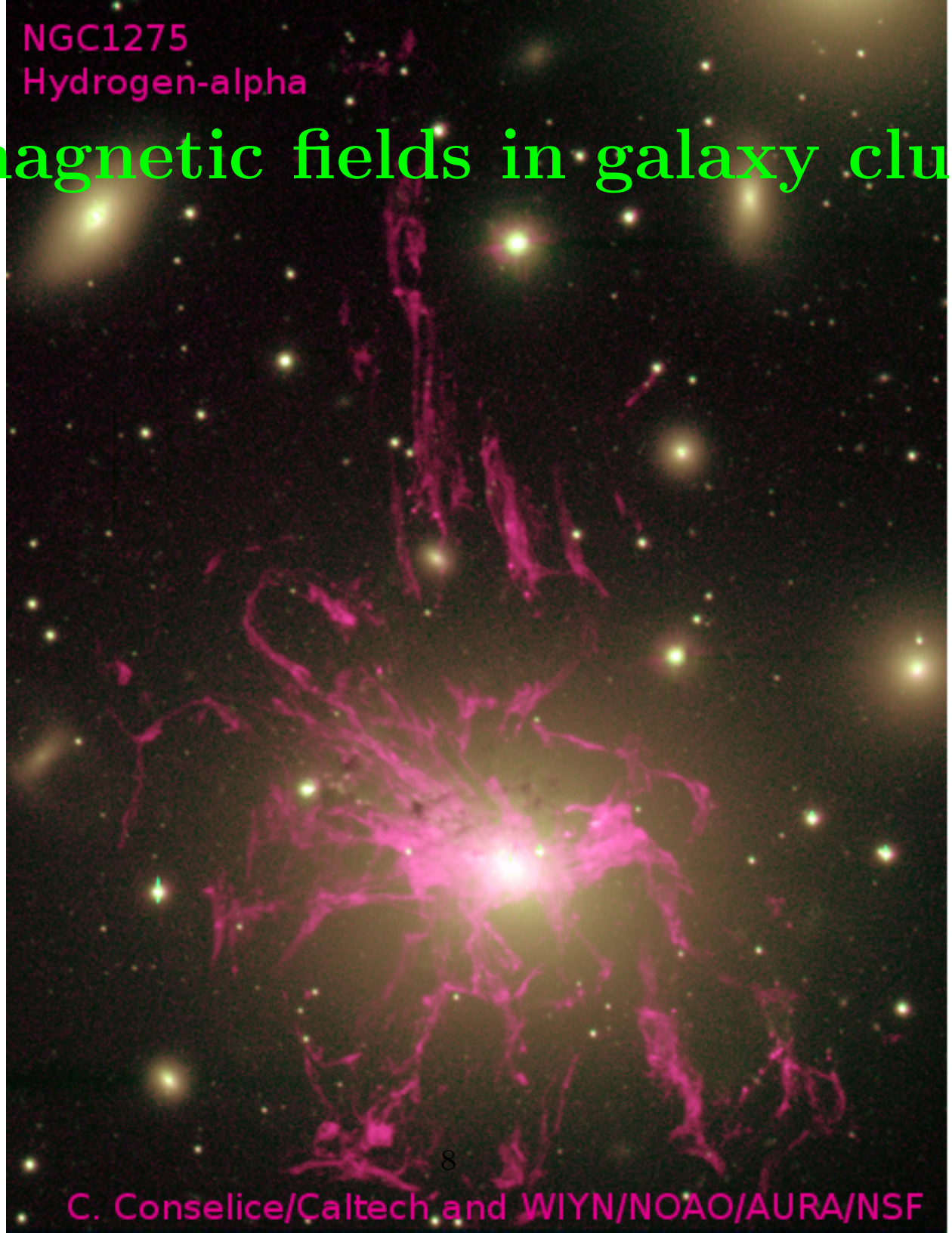

RM maps

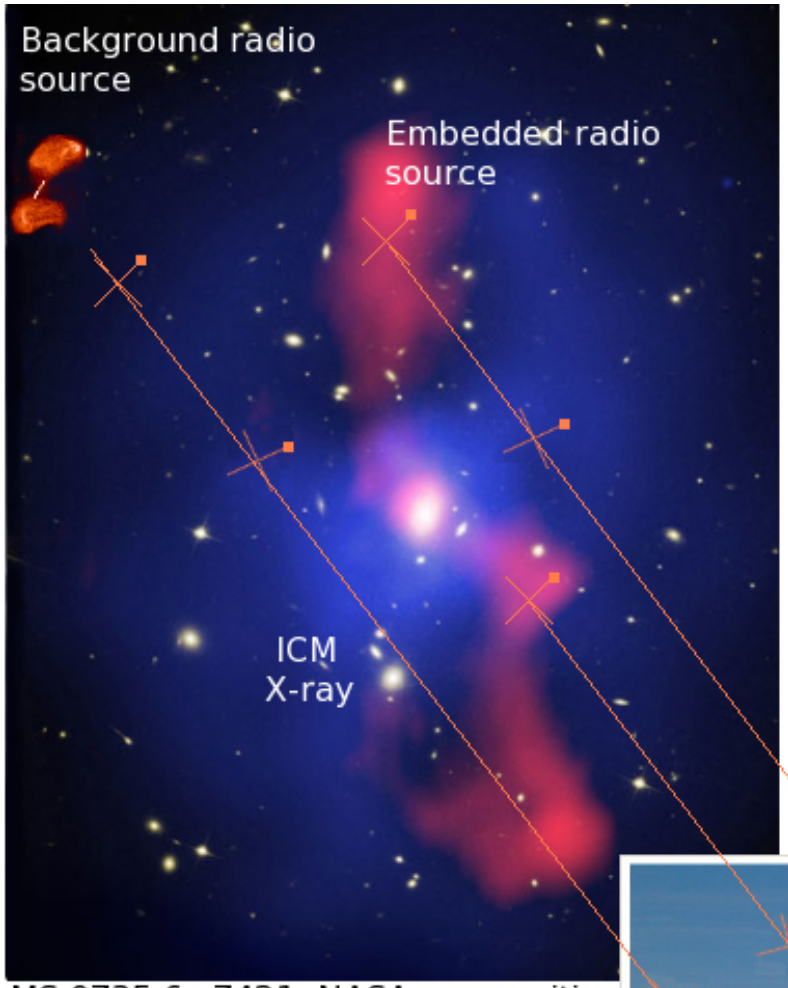

MS 0735.6+7421 NASA composition

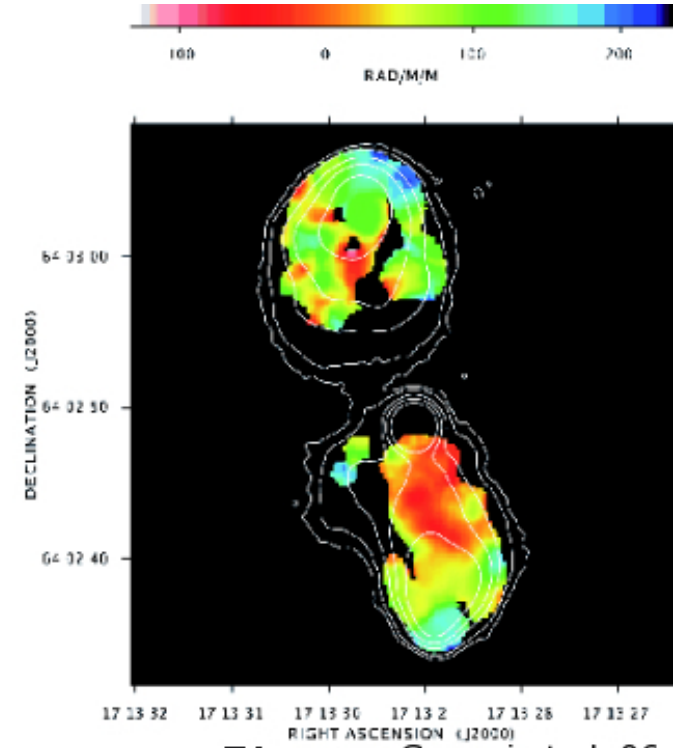

Govoni et al. 06
J1713.5+6402
Abell 2255

VLA

RM against embedded radio sources

- A23825 contains 2 extended radio galaxies
- Kolmogorov n=11/3 spectral index reproduces the data

Guidetti et al. 2007

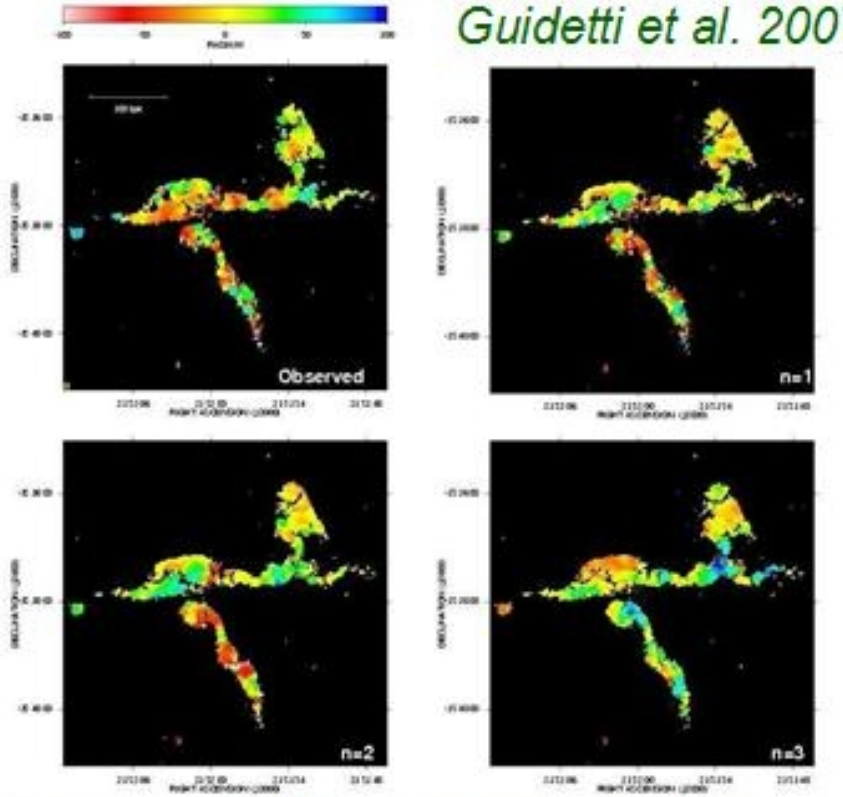

Laing Garrington effect (the further radio lobe is more depolarised)

Power-spectrum of magnetic fields

Following Tribble 1991, and Murgia et al. 2004, we generate cubes with random magnetic field distributions:

Start in Fourier space. Choose a power-law power spectrum: $|A_k|^2 \propto k^{-\zeta}$, where ζ takes the values 2, 3, 11/3 (Kolmogorov) or 4.

Draw the amplitudes A and phases ϕ of the magnetic potential vector $\tilde{\mathbf{A}}(\mathbf{k})$ randomly from: $P(A,\phi)dAd\phi = \frac{A}{2\pi|A_k|^2}\, exp\left(-\frac{A^2}{2\,|A_k|^2}\right) dAd\phi$,

Eliminate mean field, i.e., $A(k=0)=0$,

$\tilde{\mathbf{A}}(\mathbf{k}) \quad \rightarrow \quad \mathbf{A}(\mathbf{x})$,

$\mathbf{A}^{'}(\mathbf{x}) = (\mathbf{A}(\mathbf{x}) * \rho(r)_{ICM})(\mathbf{x})$, where $\rho_{ICM}(r) \propto \frac{1}{1+(r/r_c)^2}$,

$\mathbf{B}(\mathbf{x}) = \nabla \times \mathbf{A}^{'}(\mathbf{x})$, and not the other way around due to noise and

$\mathbf{B}(\mathbf{x})^{'} = B_0\, \mathbf{B}(\mathbf{x})$, so $\beta \sim 10$ everywhere.

Ideal MHD to follow the evolution

$$\frac{\partial}{\partial t}\begin{bmatrix} \rho \\ \rho v_x \\ \rho v_y \\ \rho v_z \\ \epsilon \\ B_x \\ B_y \\ B_z \end{bmatrix} + \frac{\partial}{\partial x}\begin{bmatrix} \rho v_x \\ \rho v_x^2 + P + B^2/2 - B_x^2 \\ \rho v_y v_x \\ \rho v_z v_x \\ (\epsilon + P + B^2/2)v_x - B_x(\vec{B}\cdot\vec{v}) \\ 0 \\ -E_z \\ E_y \end{bmatrix} +$$

$$\frac{\partial}{\partial y}\begin{bmatrix} \rho v_y \\ \rho v_x v_y \\ \rho v_y^2 + P + B^2/2 - B_y^2 \\ \rho v_z v_y \\ (\epsilon + P + B^2/2)v_y - B_y(\vec{B}\cdot\vec{v}) \\ E_z \\ 0 \\ -E_x \end{bmatrix} + \frac{\partial}{\partial z}\begin{bmatrix} \rho v_z \\ \rho v_x v_z \\ \rho v_y v_z \\ \rho v_z^2 + P + B^2/2 - B_z^2 \\ (\epsilon + P + B^2/2)v_y - B_z(\vec{B}\cdot\vec{v}) \\ -E_y \\ E_x \\ 0 \end{bmatrix} = \vec{S}$$

Faraday's law:

$$\frac{\partial}{\partial t}\vec{B} + \vec{\nabla} \times \vec{E} = 0, \tag{1}$$

hence, initially solenoidal magnetic field topologies remain solenoidal:

$$\vec{\nabla} \cdot \vec{B} = 0.$$

Ohm's law for a perfectly conducting medium,

$$\vec{E} = -\vec{v} \times \vec{B} \tag{2}$$

and the polytropic equation of state for an ideal gas,

$$P = (\gamma - 1)(\epsilon - \rho\vec{v}^2/2 - B^2/2). \tag{3}$$

Magnetic flux freezing

$$\frac{\partial}{\partial t}\left(\int_{S(t)} \mathbf{B}(\mathbf{r}, t) \cdot d\,\mathbf{a}\right) = 0 \tag{4}$$

We use Flash3.1 (Fryxell et al. 2000) which is an MHD, multidimensional, AMR and MPI based code.

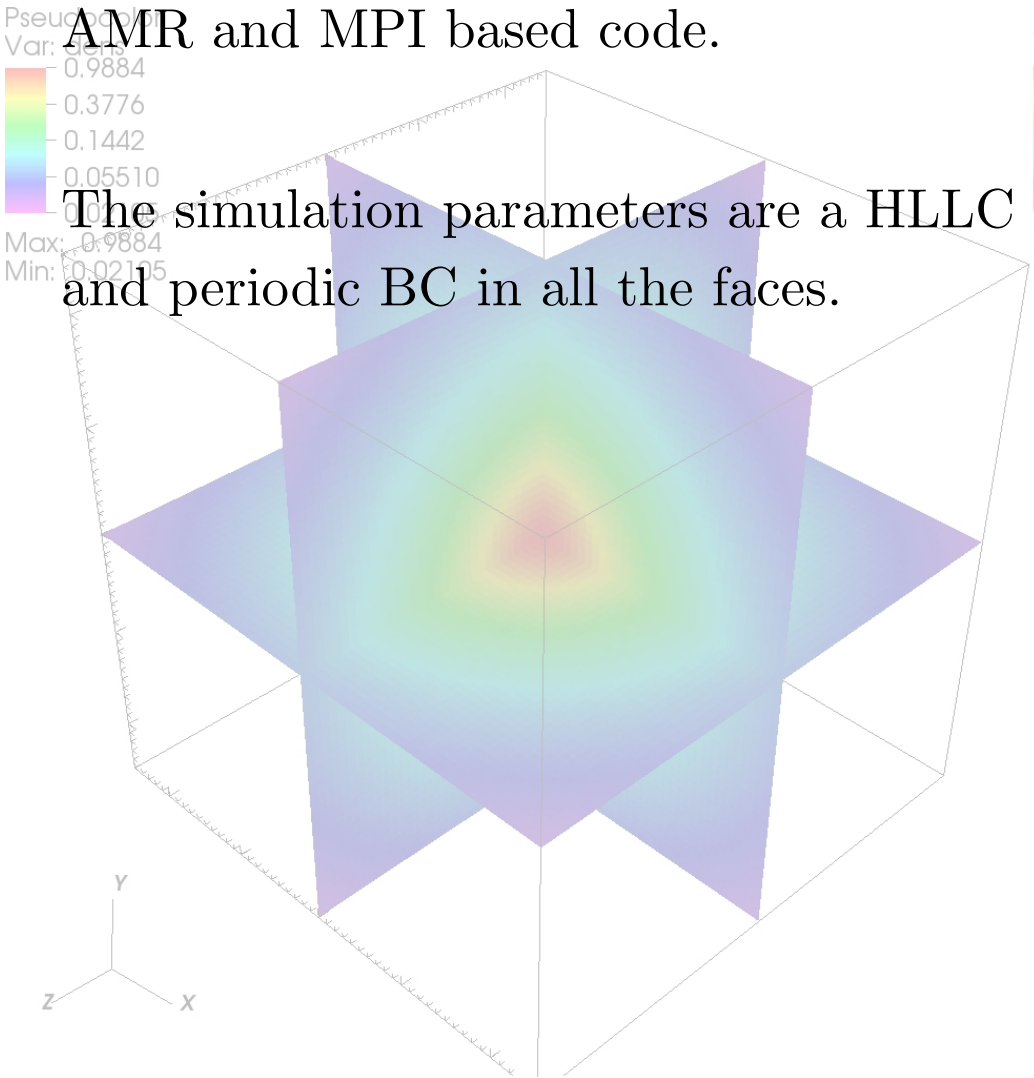

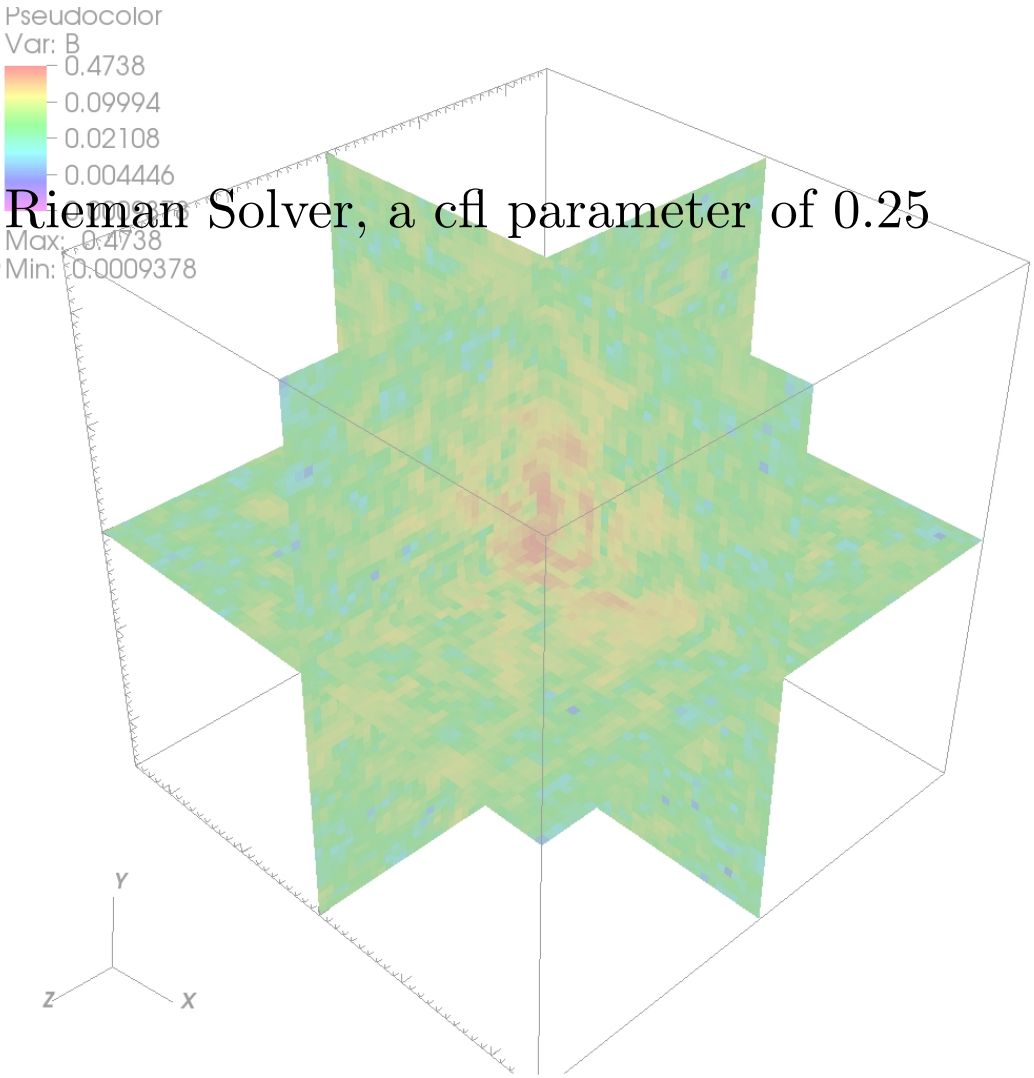

The simulation parameters are a HLLC Rieman Solver, a cfl parameter of 0.25 and periodic BC in all the faces.

We use Flash3.1 (Fryxell et al. 2000) which is an MHD, multidimensional, AMR and MPI based code.

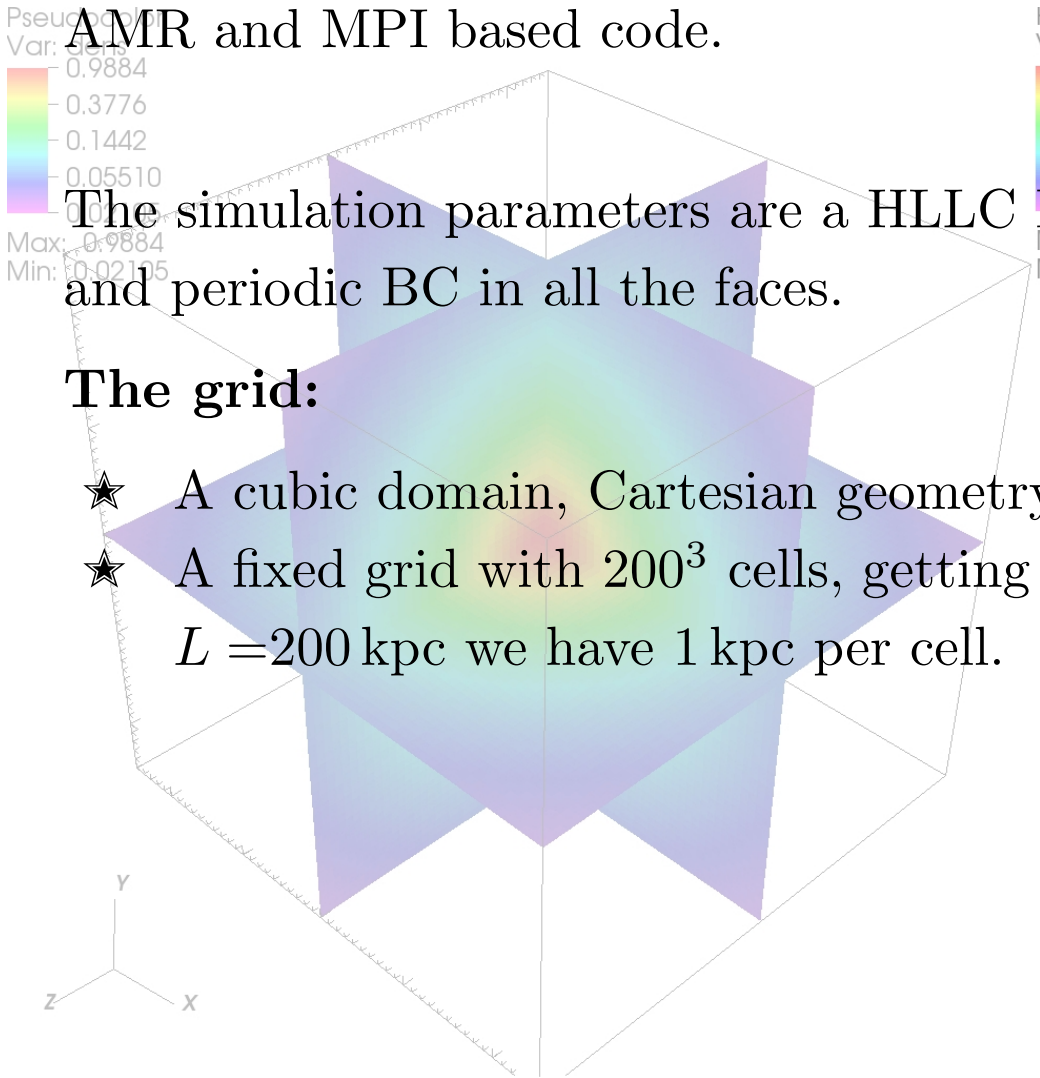

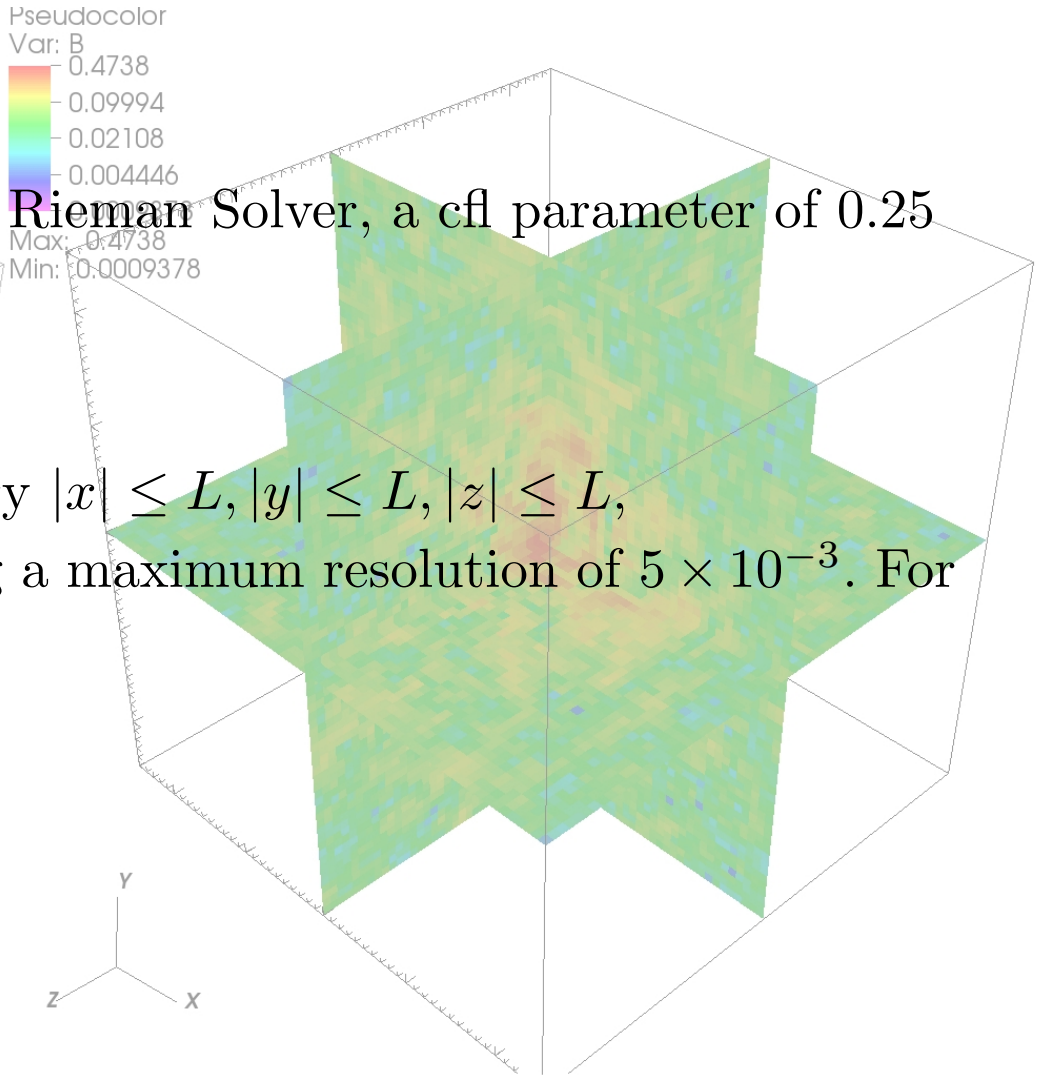

The simulation parameters are a HLLC Rieman Solver, a cfl parameter of 0.25 and periodic BC in all the faces.

The grid:

- ★ A cubic domain, Cartesian geometry $|x| \leq L, |y| \leq L, |z| \leq L$,
- ★ A fixed grid with 200^3 cells, getting a maximum resolution of 5×10^{-3}. For L =200 kpc we have 1 kpc per cell.

We use Flash3.1 (Fryxell et al. 2000) which is an MHD, multidimensional, AMR and MPI based code.

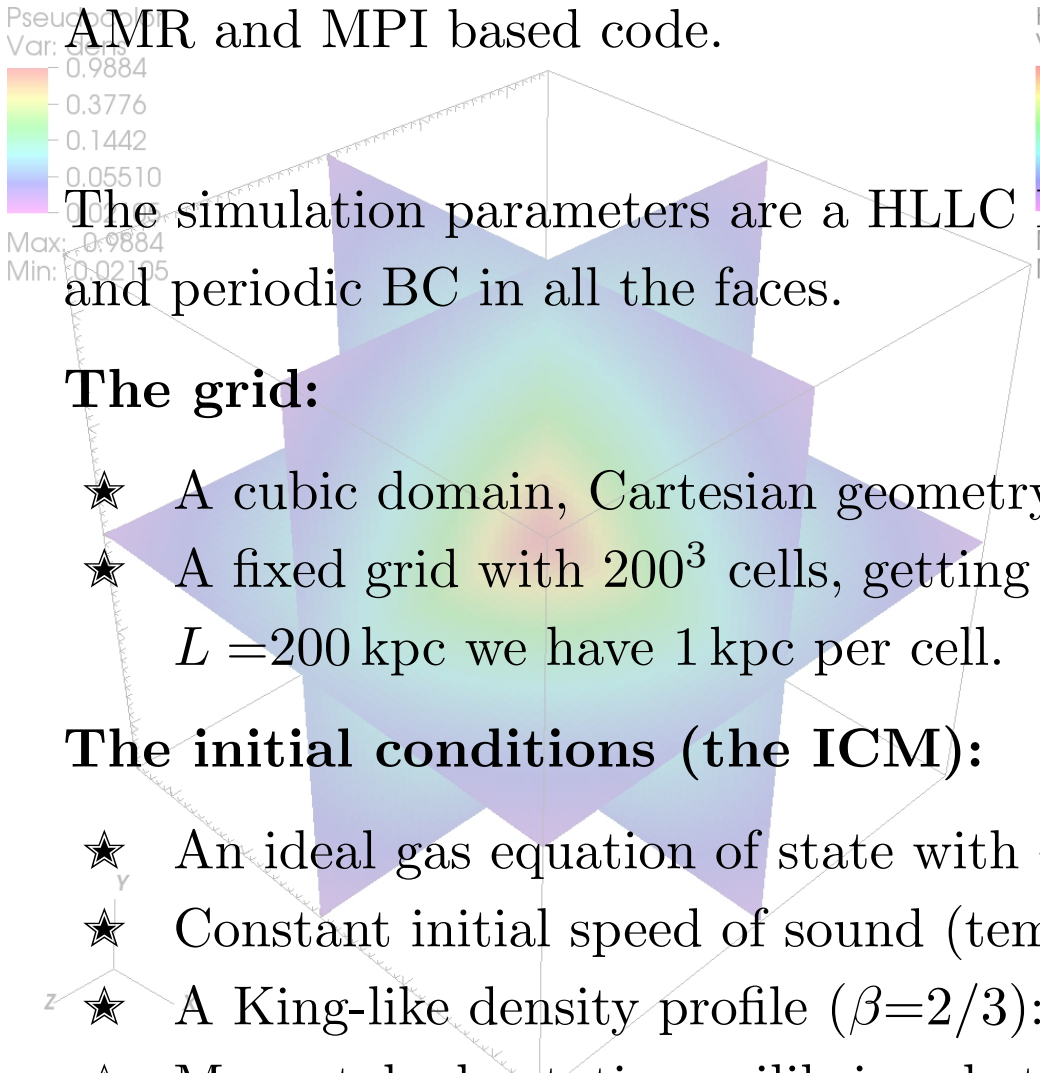

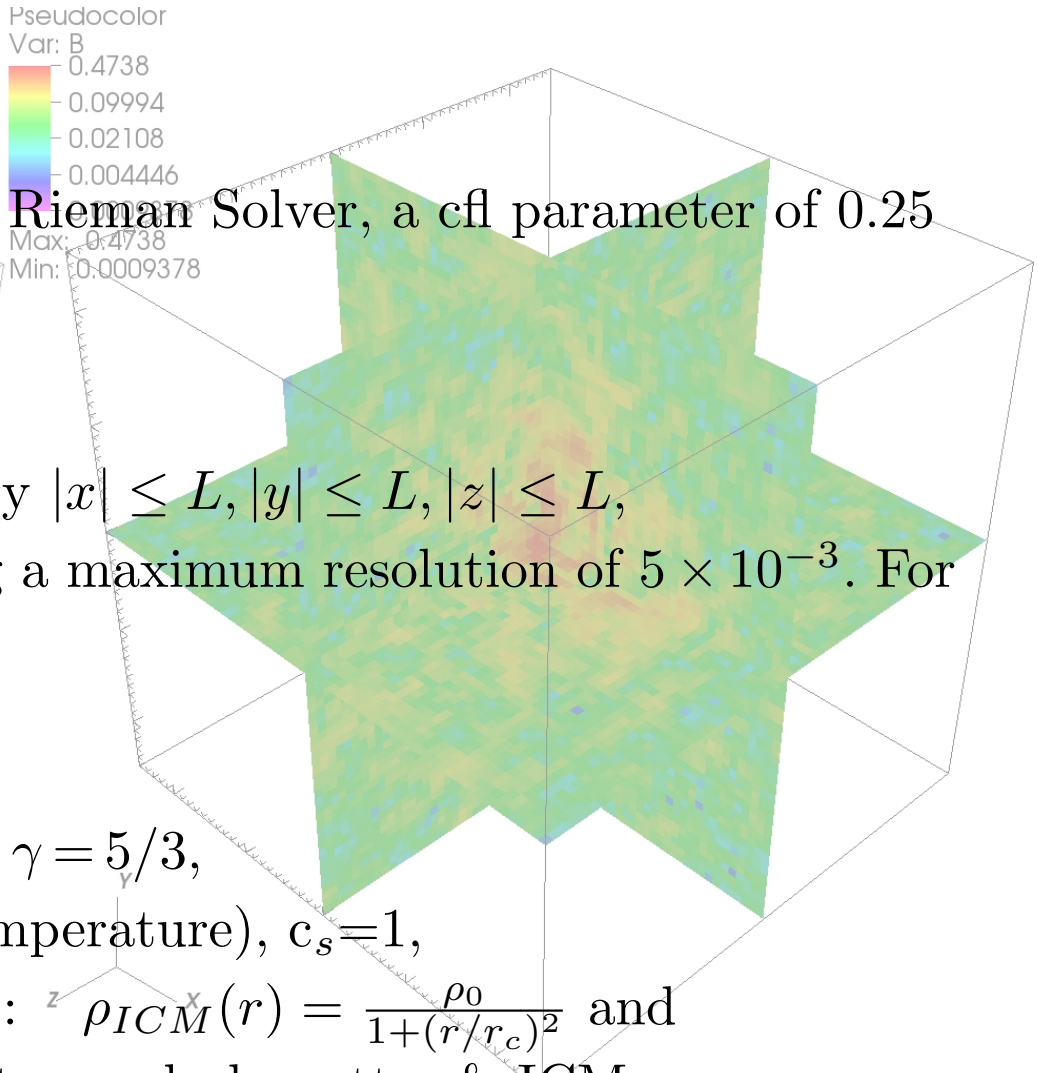

The simulation parameters are a HLLC Rieman Solver, a cfl parameter of 0.25 and periodic BC in all the faces.

The grid:

- ★ A cubic domain, Cartesian geometry $|x| \leq L, |y| \leq L, |z| \leq L$,
- ★ A fixed grid with 200^3 cells, getting a maximum resolution of 5×10^{-3}. For L =200 kpc we have 1 kpc per cell.

The initial conditions (the ICM):

- ★ An ideal gas equation of state with $\gamma = 5/3$,
- ★ Constant initial speed of sound (temperature), c_s=1,
- ★ A King-like density profile (β=2/3): $\rho_{ICM}(r) = \frac{\rho_0}{1+(r/r_c)^2}$ and
- ★ Magnetohydrostatic equilibrium between dark matter & ICM pressure: $g_r = -\frac{2\,c_s^2}{\gamma\,a_0^2} \frac{r}{(1+(r/a_0)^2)} \left(1 + \frac{1}{\beta_m}\right)$.

The Jets

We inject mass and energy into a central cylinder in the grid:

$$\begin{aligned}
\rho^{n+1}_{x,\text{nozzle}} &= \rho^{n}_{x,\text{nozzle}} + \dot{\rho}_j \, dt \\
&= \rho^{n}_{x,\text{nozzle}} + \delta(\mathbf{x}, t) \, \frac{\eta \rho_0}{t_m} \, dt, \\
v^{n+1}_{x,\text{nozzle}} &= v^{n}_{x,\text{nozzle}} + \dot{v}_j \, dt \\
&= v^{n}_{x,\text{nozzle}} + \delta(\mathbf{x}, t) \, \frac{v_j}{t_k} \, dt,
\end{aligned}$$

respectively, where

$$\delta(\mathbf{x}, t) = \begin{cases} 1 & \text{for} \quad |\mathbf{x}| \leq l_j \text{ and } t \in (t_s, t_e); \\ 0 & \text{otherwise,} \end{cases}$$

η is the jets vs ambient density contrast, v_j is the jets' velocity, t_m and t_k are the mass and energy injection rates, respectively, and t_j characterises the duration of the injection.

Parameter space:

Jets velocity [Mach]	Jets vs ambient density contrast	Jets power [W]
40	0.001	3.8×10^{38}
40	0.01	1.6×10^{39}
80	0.001	1.5×10^{39}
80	0.01	1.1×10^{40}

$$t_{\rm simul} \propto \frac{1}{n_{\rm processors}} \frac{\Delta x}{\vec{v}_{\rm relevant}} + t_{\rm queue} \sim \text{4–12 hours} \quad \text{with 64–128 proc.}$$

For the analysis, rescale to units in the high energy extragalactic context:

$\rho_0 = 1 \times 10^{-2}$ cm^{-3},
$L = 200$ kpc,
$< \mathbf{B} > \in (1, 100)\, \mu$Gauss and
$c_s \sim 1.6 \times 10^8$ cm s^{-1}, for a plasma temperature of $\sim 10^8$ K.

Synthetic RM maps of the AGN feedback on the cluster magnetic fields:

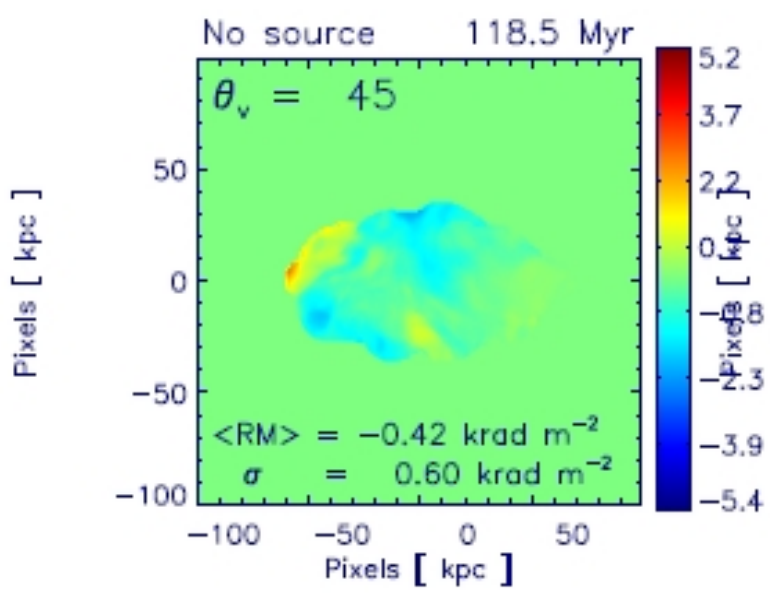

(a)

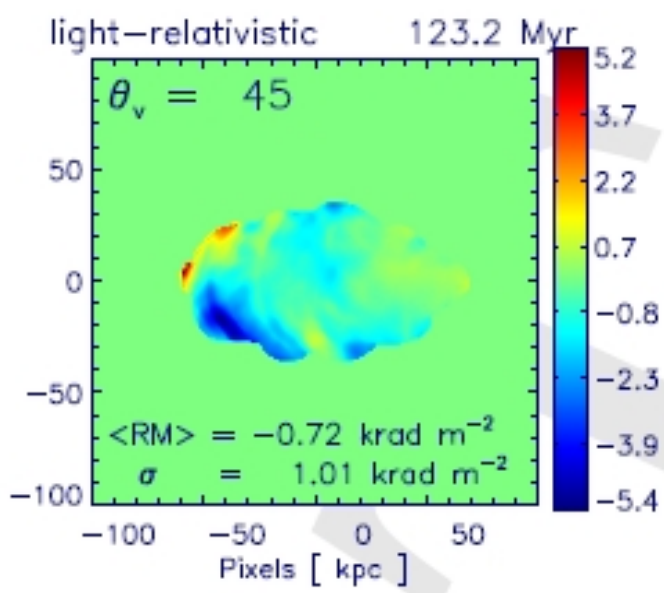

(b)

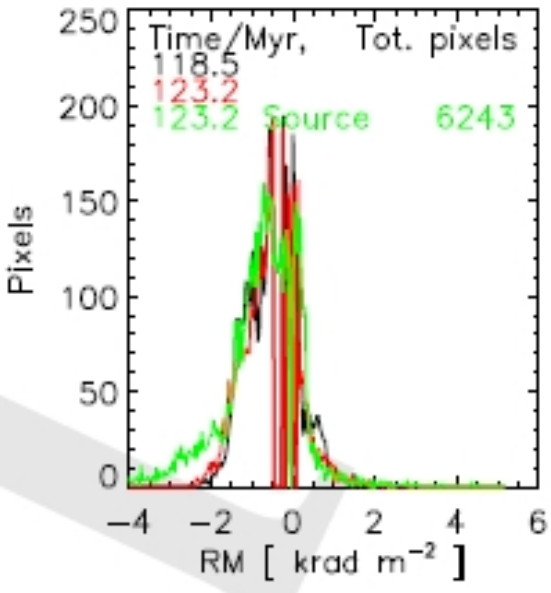

(c)

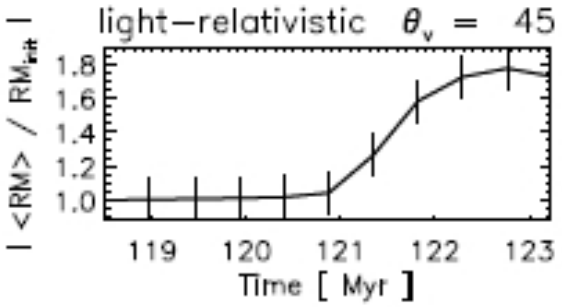

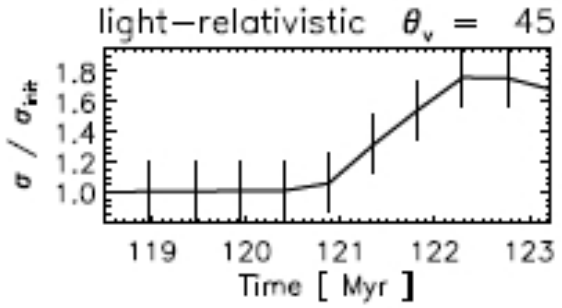

(d)

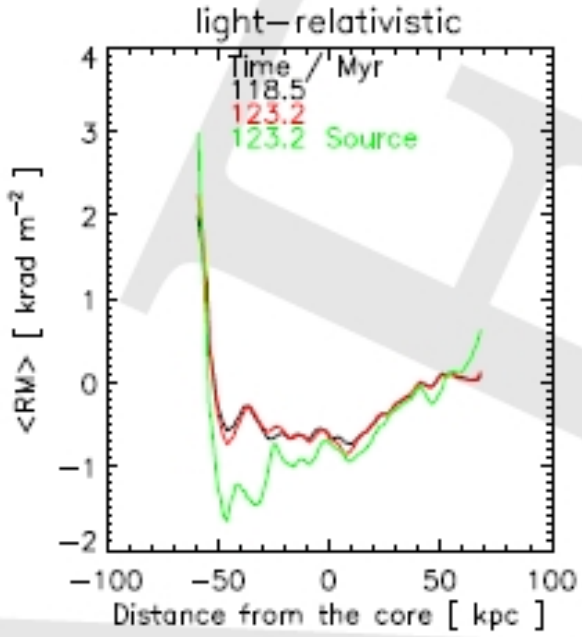

(e)

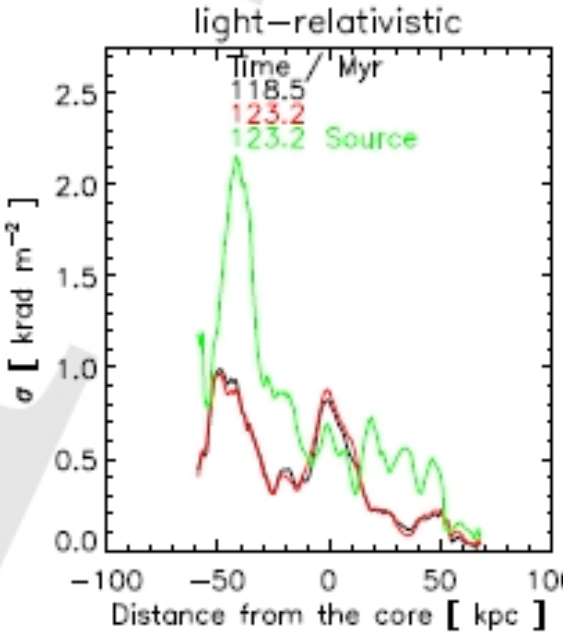

(f)

The topology of the magnetic fields lines 12 Myr after the relaxation:

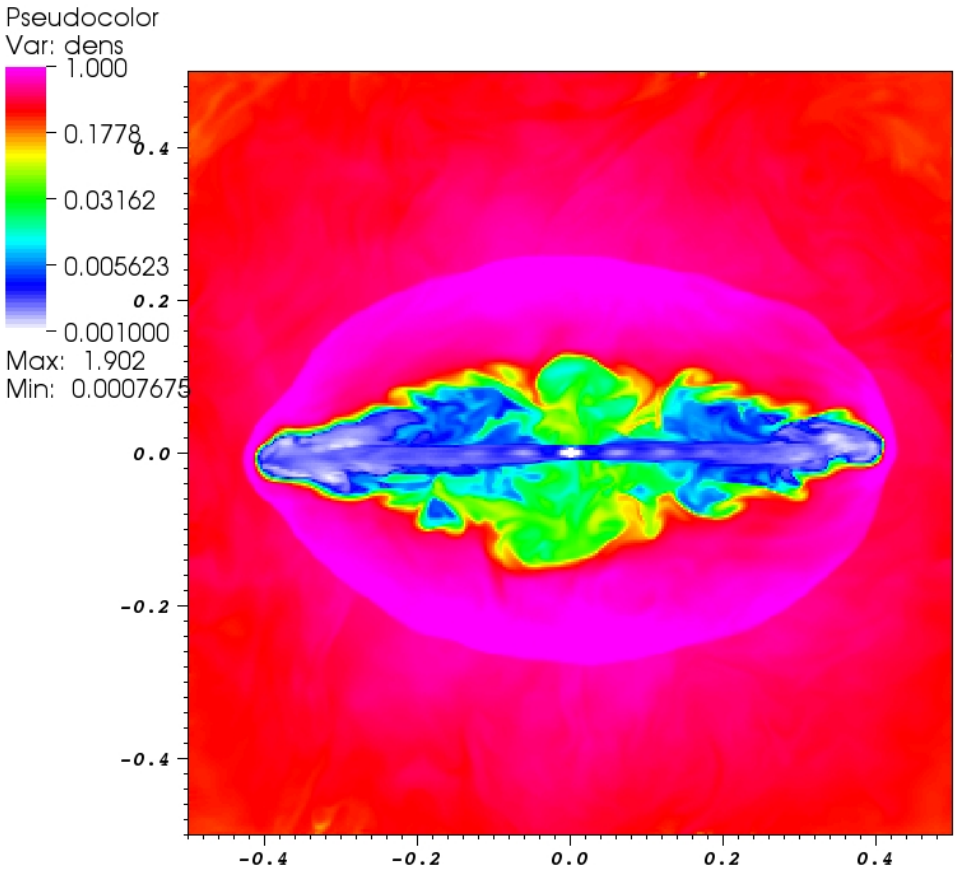

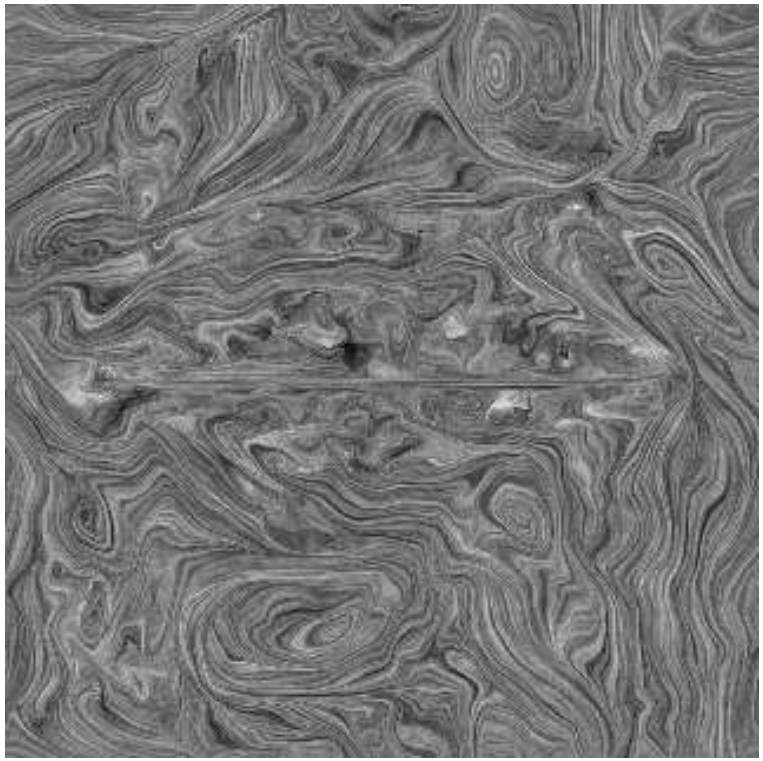

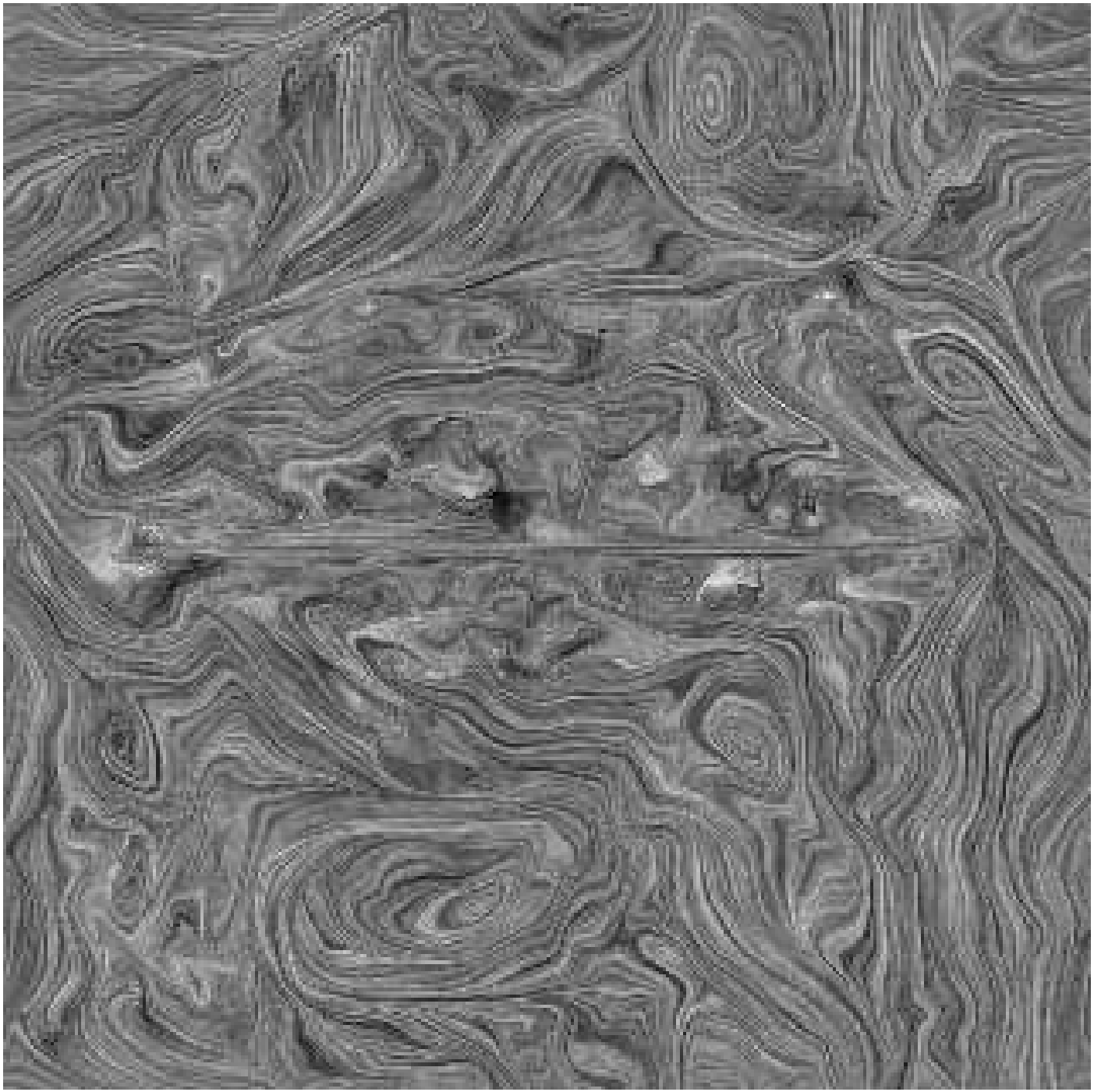

Synthetic maps of non-thermal polarized synchrotron emission.

Data cubes $\longrightarrow$ Stokes parameters (for each cell):

$$I = \left\langle E_x^2 + E_y^2 \right\rangle, \quad Q = \left\langle E_x^2 - E_y^2 \right\rangle, \quad U = \langle 2E_x E_y \cos(\psi_x - \psi_y) \rangle \qquad (5)$$

where $\langle\,\rangle$ denotes ensemble-averaing though the source, along the line of sight, and I respresents the polarisation intesity of the radiation.

In terms of these parameters:
The polarisation angle $\chi_B = \arctan(U/Q)/2 + \pi/2$ and
the degree of polarisation $d_p = \sqrt{U^2 + Q^2}/I$.

Which one is the observation?

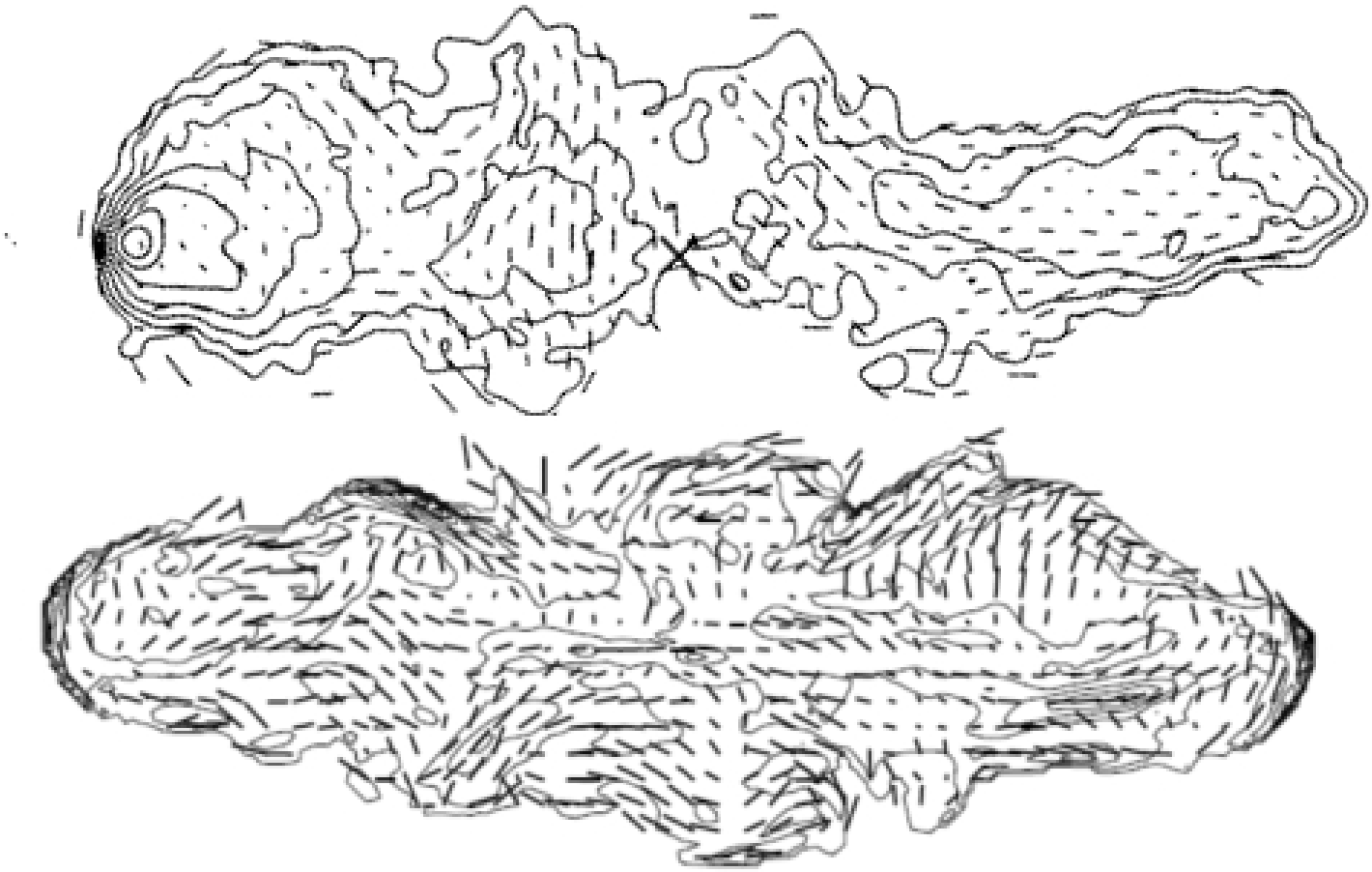

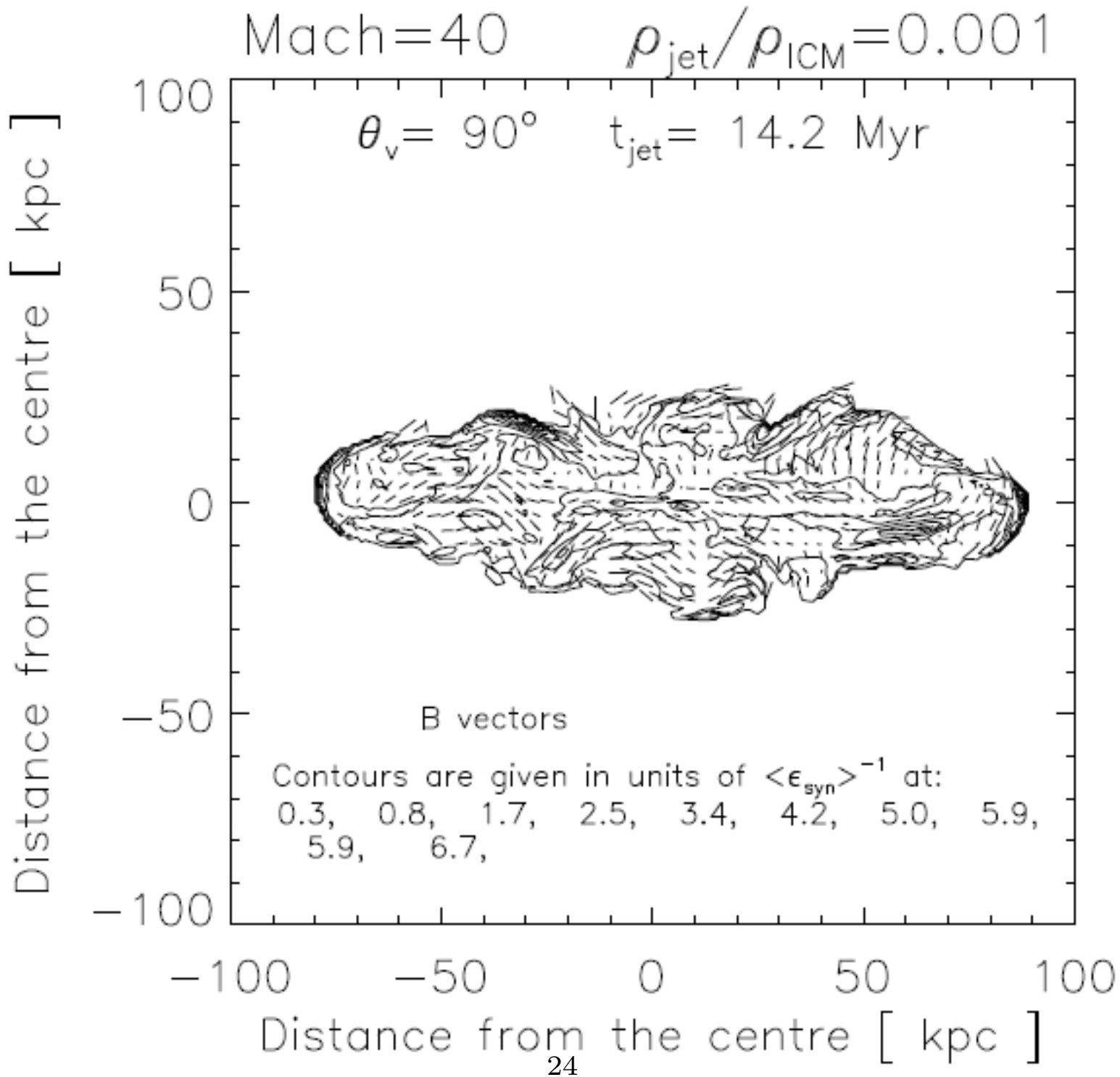
Mach=40
ρ_{jet}/ρ_{ICM}=0.001
θ_v= 90°
t_{jet}= 14.2 Myr
B vectors
Contours are given in units of $<\epsilon_{syn}>^{-1}$ at:
0.3, 0.8, 1.7, 2.5, 3.4, 4.2, 5.0, 5.9,
5.9, 6.7,
Distance from the centre [kpc]
Distance from the centre [kpc]
100
50
0
−50
−100
−100
−50
0
50
100

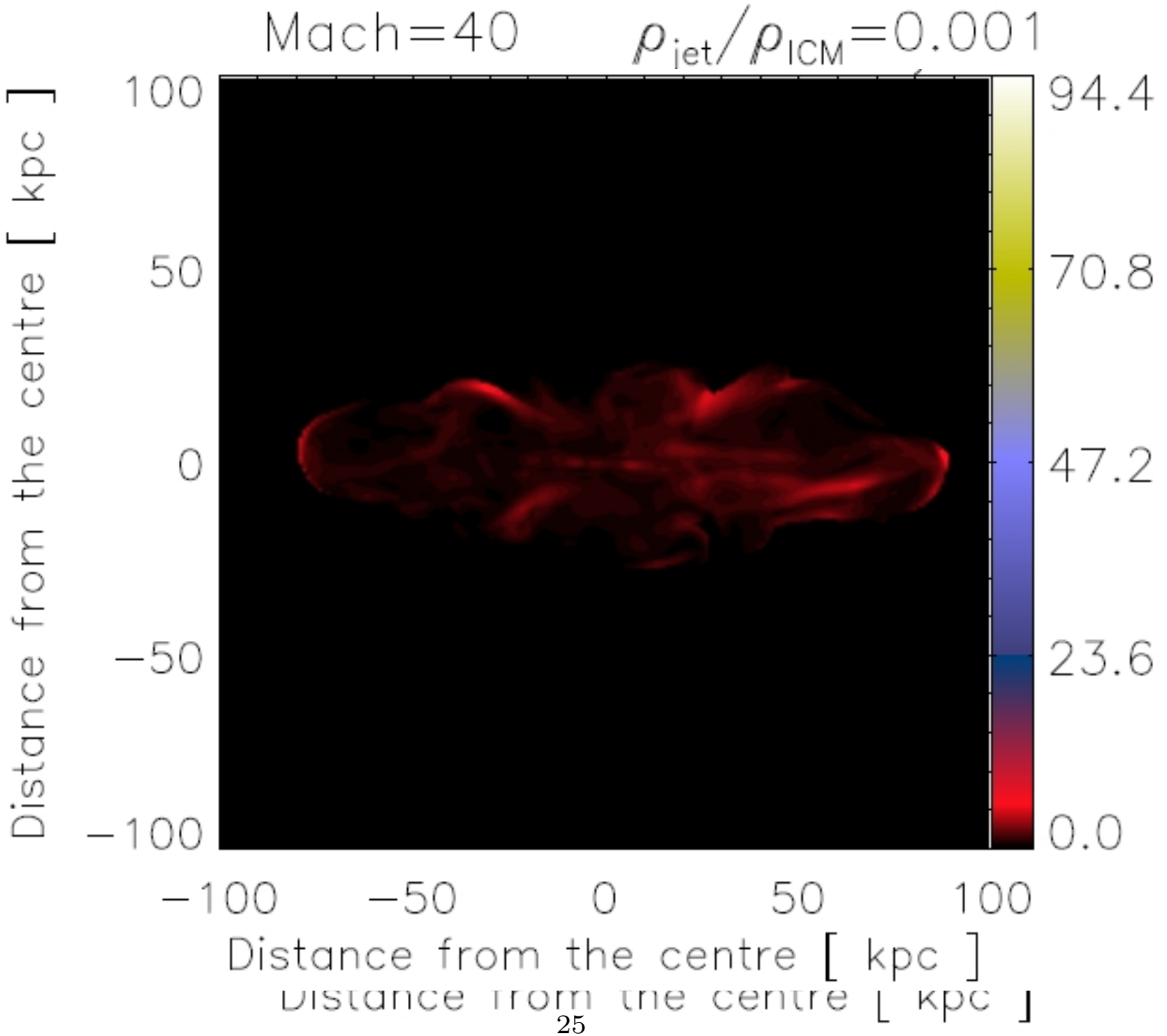
Mach=40
ρ_{jet}/ρ_{ICM}=0.001
100
50
0
−50
−100
94.4
70.8
47.2
23.6
0.0
Distance from the centre [kpc]
−100
−50
0
50
100
Distance from the centre [kpc]

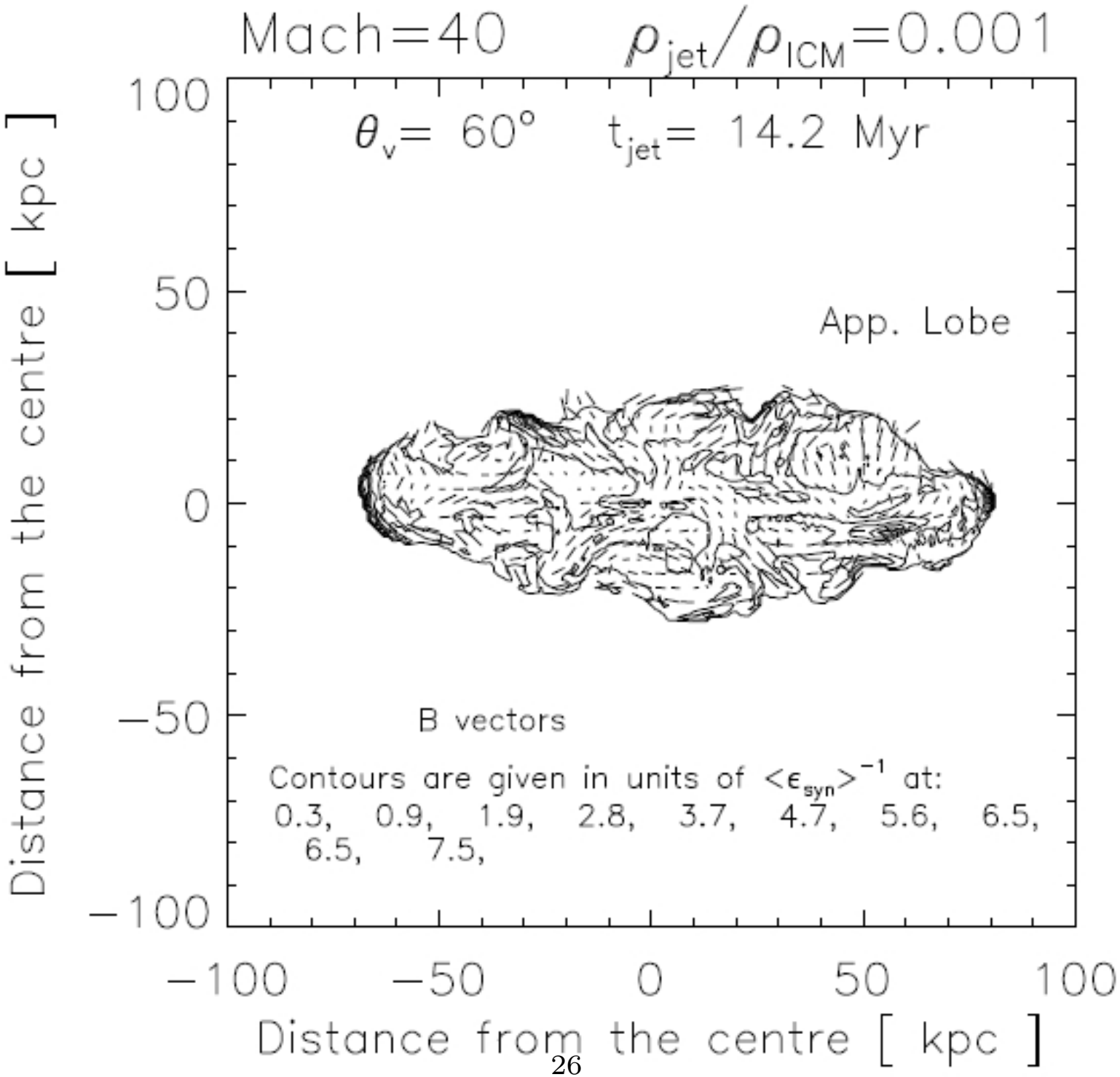
Mach=40
ρ_{jet}/ρ_{ICM}=0.001
θ_v= 60°
t_{jet}= 14.2 Myr
App. Lobe
B vectors
Contours are given in units of $<\epsilon_{syn}>^{-1}$ at:
0.3, 0.9, 1.9, 2.8, 3.7, 4.7, 5.6, 6.5,
6.5, 7.5,
100
50
0
−50
−100
−100
−50
0
50
100
Distance from the centre [kpc]
Distance from the centre [kpc]

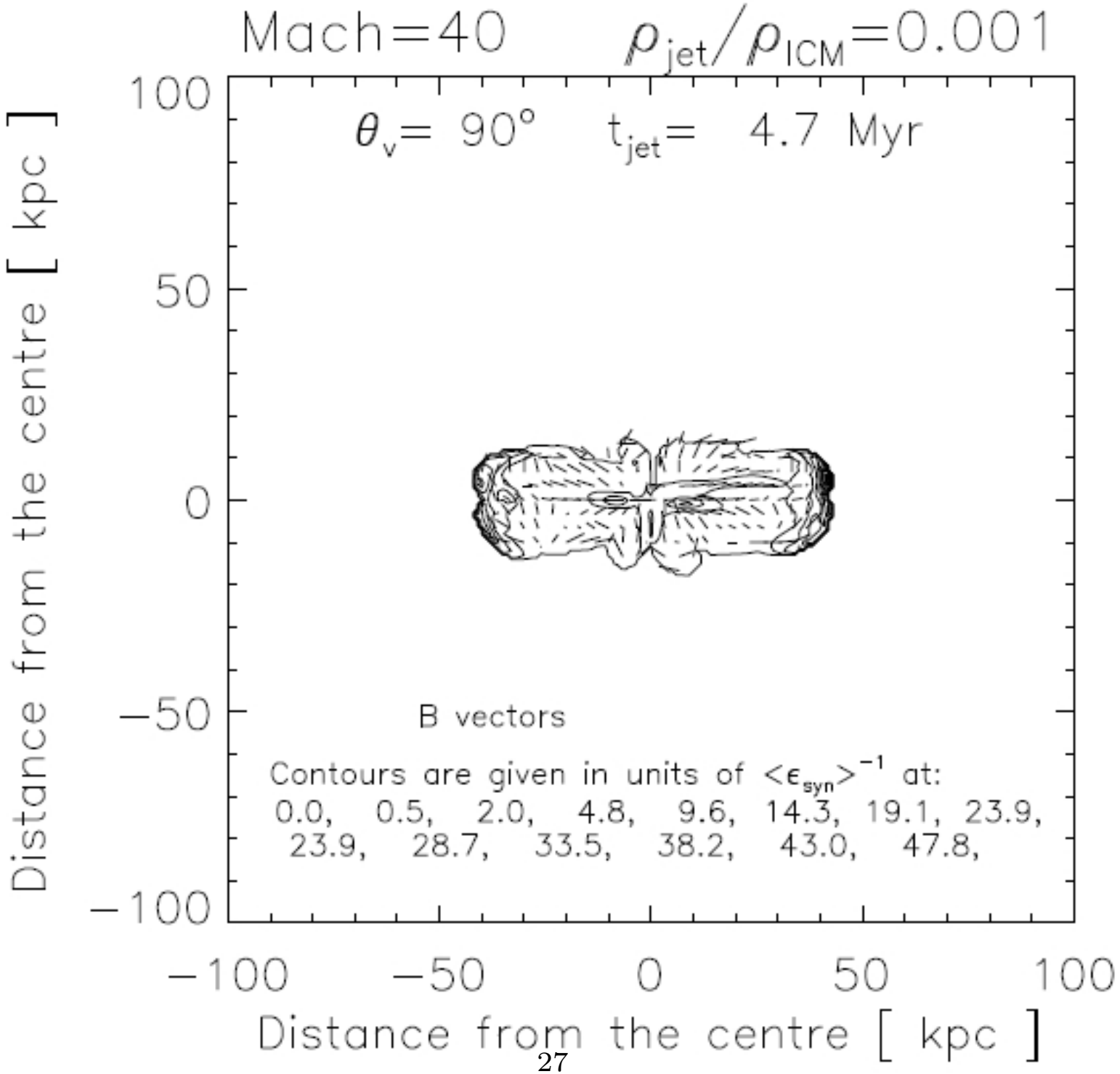
Mach=40
ρ_{jet}/ρ_{ICM}=0.001
θ_v= 90°
t_{jet}= 4.7 Myr
B vectors
Contours are given in units of $<\epsilon_{syn}>^{-1}$ at:
0.0, 0.5, 2.0, 4.8, 9.6, 14.3, 19.1, 23.9,
23.9, 28.7, 33.5, 38.2, 43.0, 47.8,
100
50
0
−50
−100
−100 −50 0 50 100
Distance from the centre [kpc]
Distance from the centre [kpc]

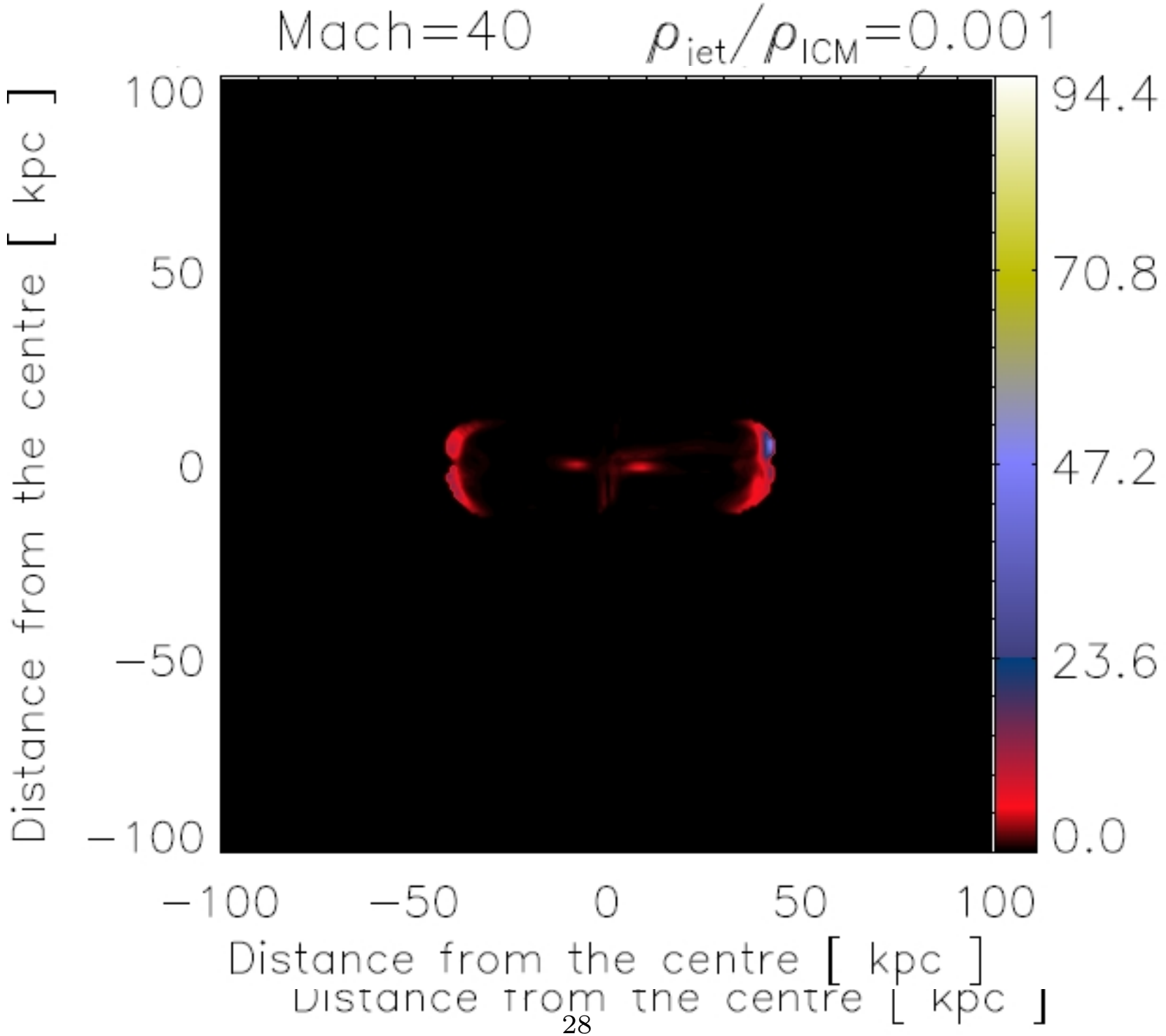
Mach=40
ρ_{jet}/ρ_{ICM}=0.001
100
50
0
−50
−100
94.4
70.8
47.2
23.6
0.0
−100
−50
0
50
100
Distance from the centre [kpc]
Distance from the centre [kpc]
Distance from the centre [kpc]

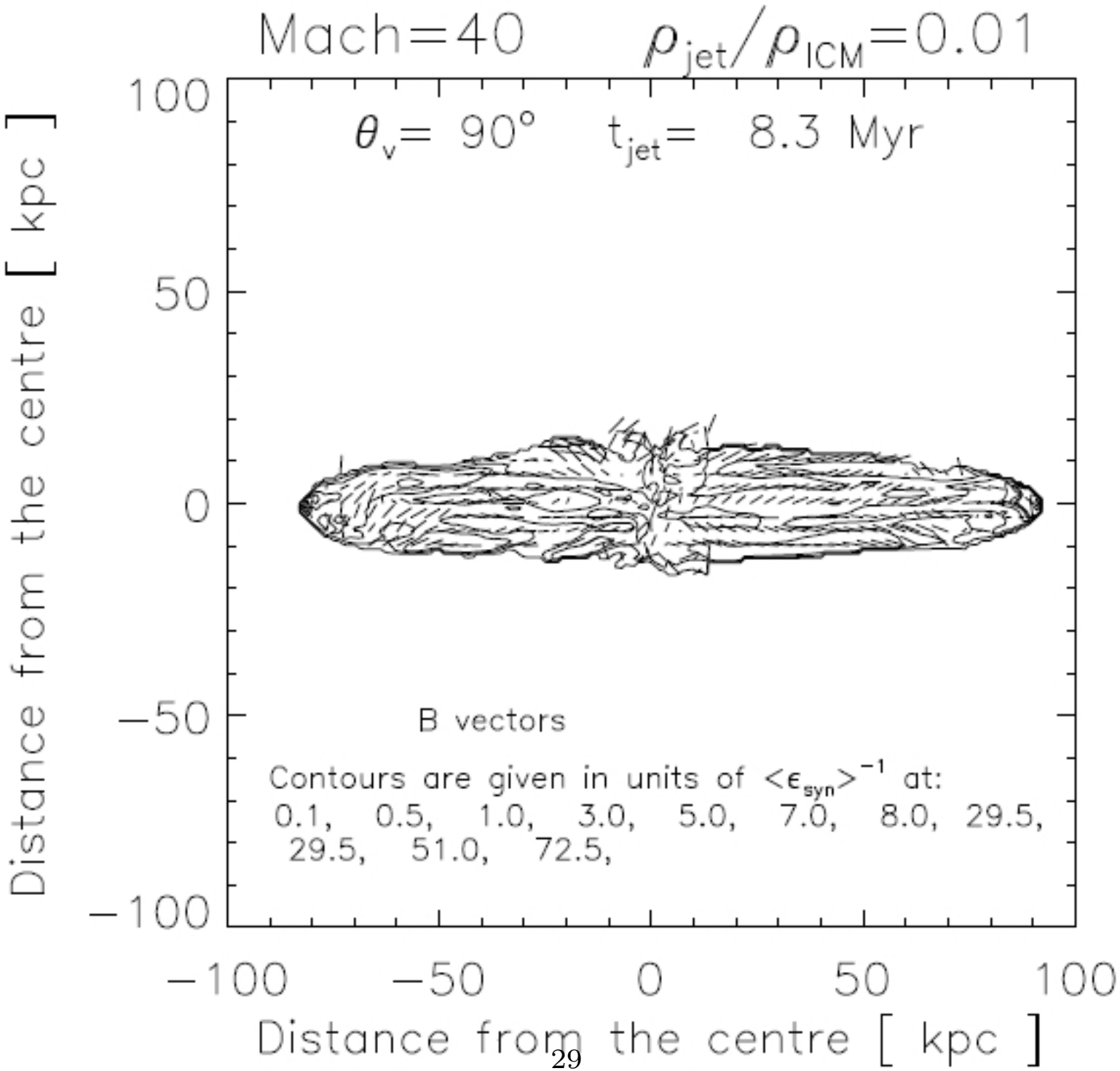
Mach=40
ρ_{jet}/ρ_{ICM}=0.01
θ_v= 90°
t_{jet}= 8.3 Myr
B vectors
Contours are given in units of $<\epsilon_{syn}>^{-1}$ at:
0.1, 0.5, 1.0, 3.0, 5.0, 7.0, 8.0, 29.5,
29.5, 51.0, 72.5,
Distance from the centre [kpc]
Distance from the centre [kpc]
100
50
0
−50
−100
−100
−50
0
50
100

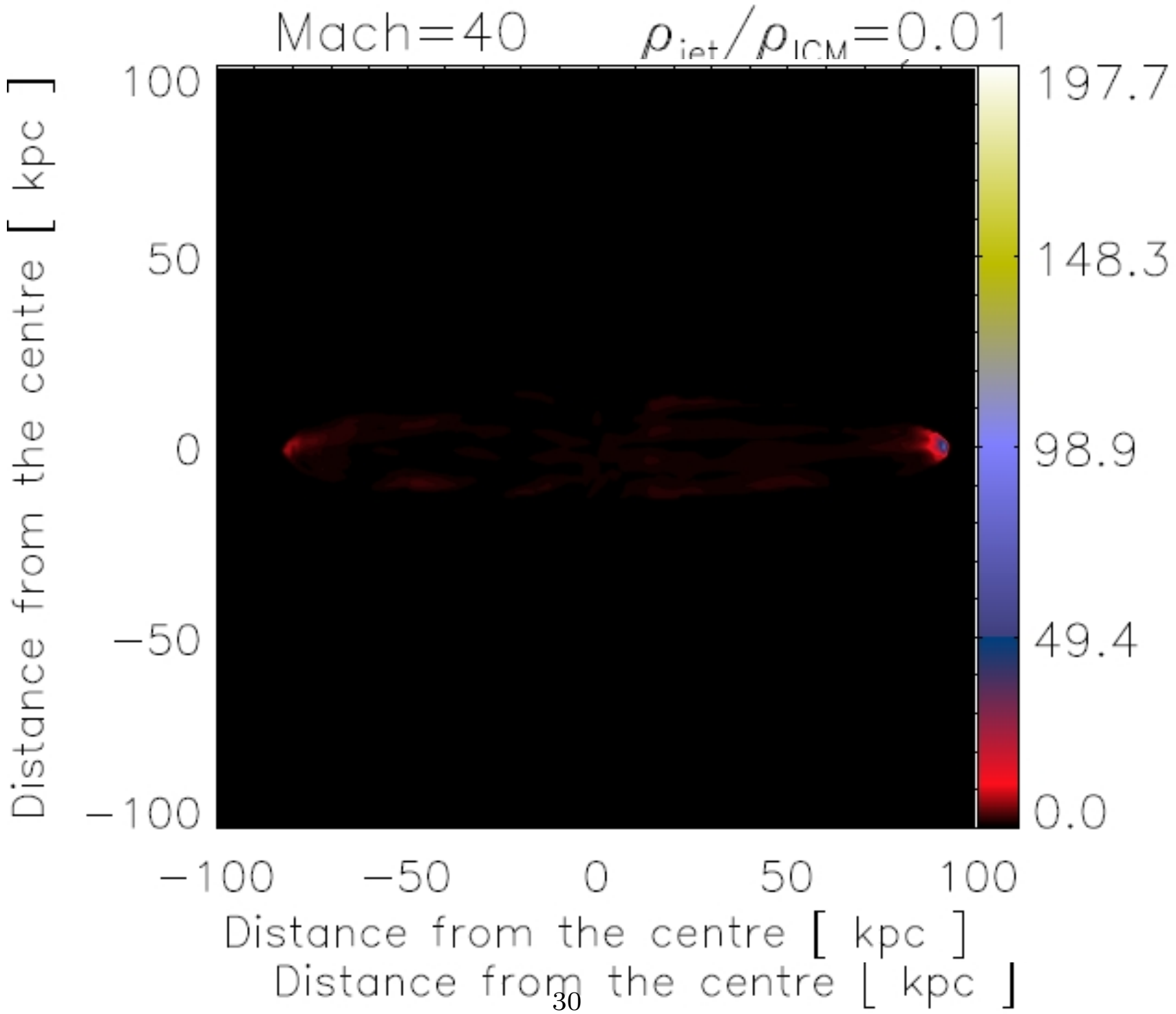
Mach=40
ρ_{jet}/ρ_{ICM}=0.01
100
50
0
−50
−100
197.7
148.3
98.9
49.4
0.0
−100
−50
0
50
100
Distance from the centre [kpc]
Distance from the centre [kpc]
Distance from the centre [kpc]

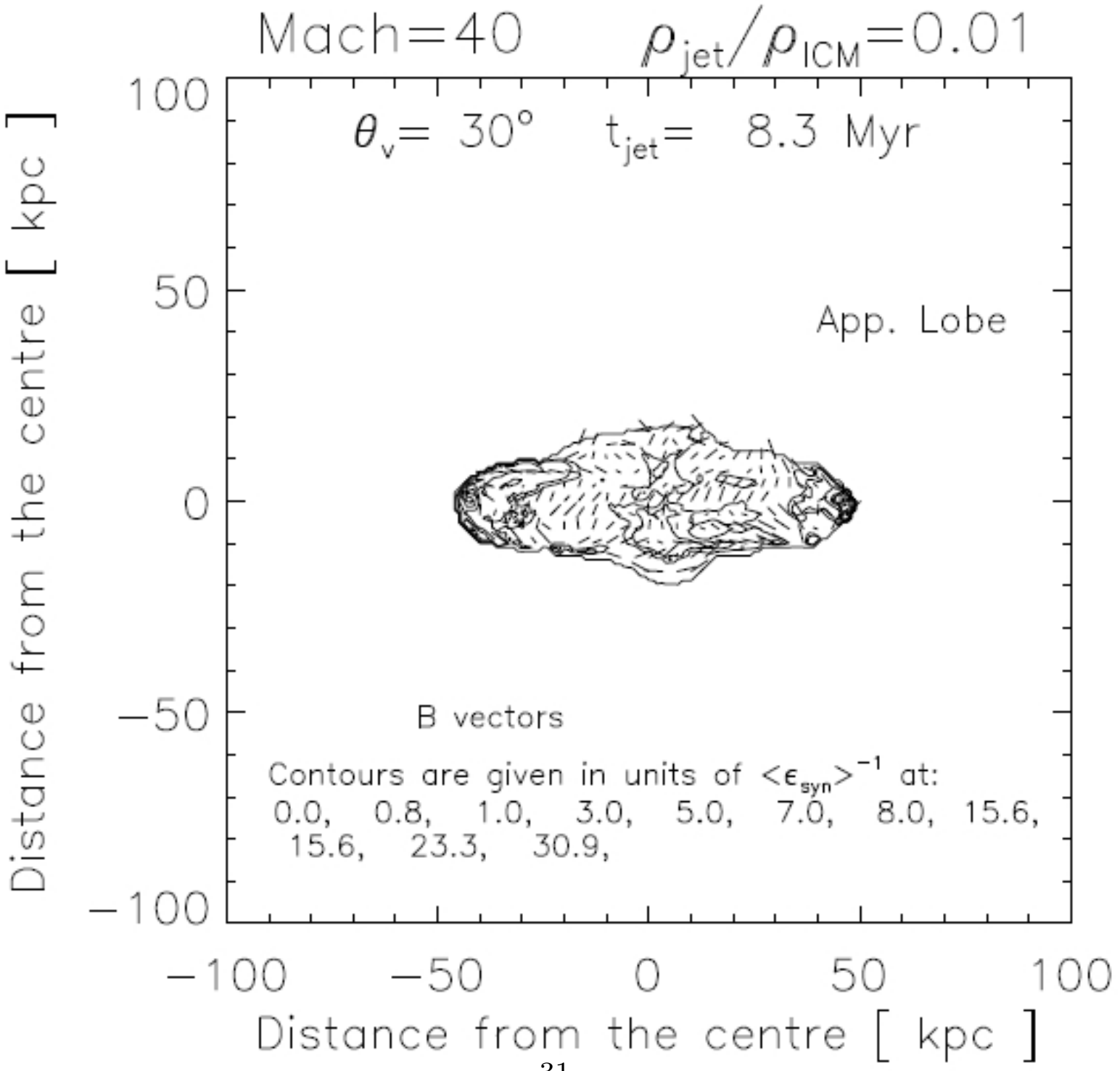
Mach=40
ρ_{jet}/ρ_{ICM}=0.01
θ_v= 30°
t_{jet}= 8.3 Myr
App. Lobe
B vectors
Contours are given in units of $<\epsilon_{syn}>^{-1}$ at:
0.0, 0.8, 1.0, 3.0, 5.0, 7.0, 8.0, 15.6,
15.6, 23.3, 30.9,
Distance from the centre [kpc]
Distance from the centre [kpc]
100
50
0
−50
−100
−100
−50
0
50
100

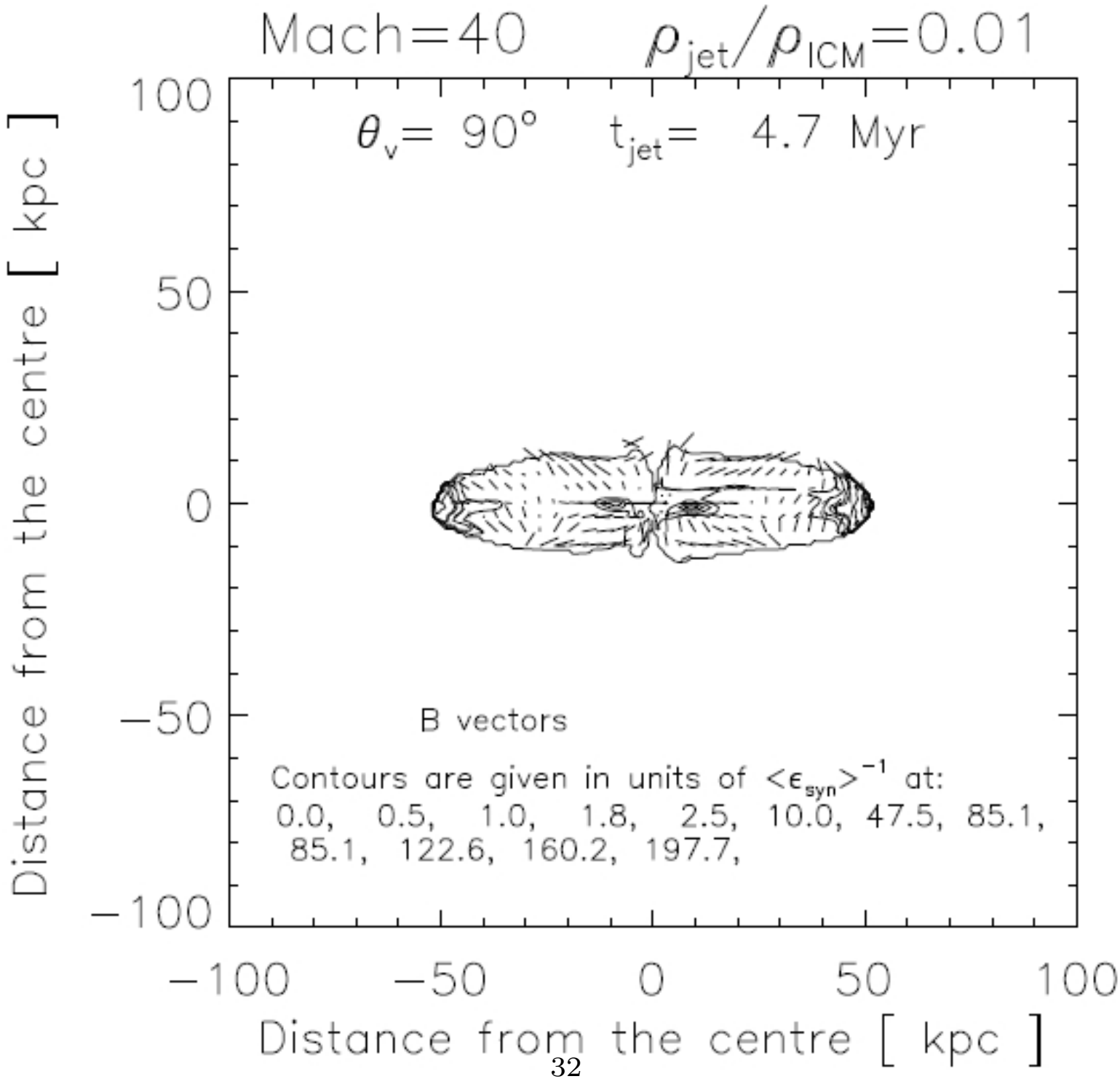
Mach=40
ρ_{jet}/ρ_{ICM}=0.01
θ_v= 90°
t_{jet}= 4.7 Myr
B vectors
Contours are given in units of $<\epsilon_{syn}>^{-1}$ at:
0.0, 0.5, 1.0, 1.8, 2.5, 10.0, 47.5, 85.1,
85.1, 122.6, 160.2, 197.7,
Distance from the centre [kpc]
Distance from the centre [kpc]
100
50
0
−50
−100
−100
−50
0
50
100

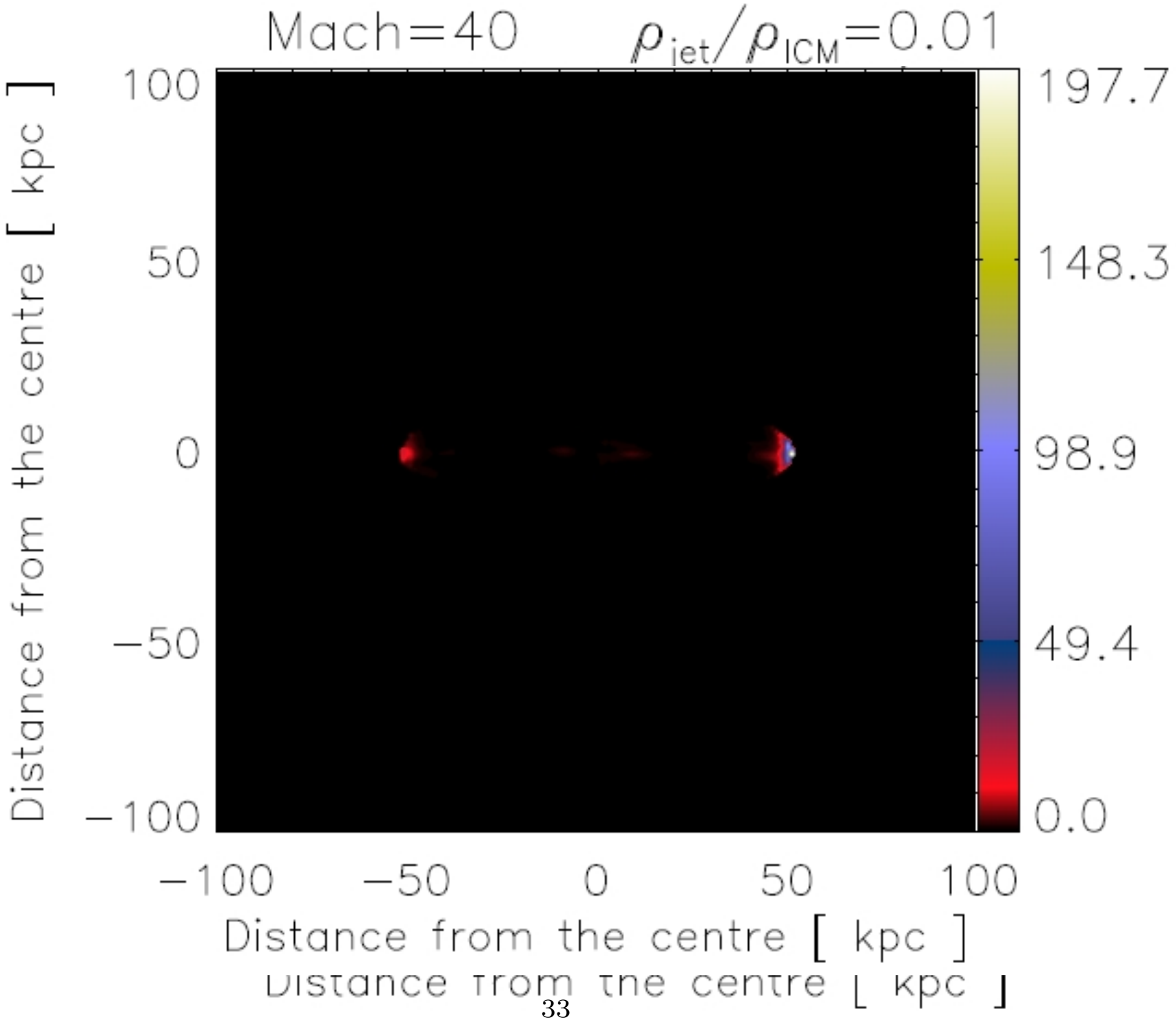
Mach=40
ρ_{jet}/ρ_{ICM}=0.01
100
50
0
−50
−100
197.7
148.3
98.9
49.4
0.0
−100
−50
0
50
100
Distance from the centre [kpc]
Distance from the centre [kpc]
Distance from the centre [kpc]

Summary and discussion

- ✯ $\chi_B \sim 90°$ along the jets' projection, but it is typically higher elsewhere.
  Consistent with topology maps and magnetic flux freezing.
  Little dependence with time.
- ✯ χ_B seems bipolar when jets have $\eta = 0.01$, but not clear trends for $\eta = 0.001$.
  Correlation with sources morphology and energy distribution.
- ✯ The outermost B-vectors are generally tangent to the dimmest emissivity contours.
  $\sim$ uniform B-vectors distribution close to shocks but not elsewhere.
- ✯ At 90° and 60° the polarisation maps are quite similar but not for 30°.
  Though to observe.
- ✯ Lots of work to do: couple with RM maps; PD diagrams (luminosity vs size); depolarization; composition of AGN plasma; resolution study; etc.

Summary and discussion

- ★ $\chi_B \sim 90°$ along the jets' projection, but it is typically higher elsewhere.
  Consistent with topology maps and magnetic flux freezing.
  Little dependence with time.
- ★ χ_B seems bipolar when jets have $\eta = 0.01$, but not clear trends for $\eta = 0.001$.
  Correlation with sources morphology and energy distribution.
- ★ The outermost B-vectors are generally tangent to the dimmest emissivity contours.
  $\sim$ uniform B-vectors distribution close to shocks but not elsewhere.
- ★ At 90° and 60° the polarisation maps are quite similar but not for 30°.
  Though to observe.
- ★ Lots of work to do: couple with RM maps; PD diagrams (luminosity vs size); depolarization; composition of AGN plasma; resolution study; etc.

Thanks!

Movies @ *h*ttp://www.mrao.cam.ac.uk/∼mh475/.

Talk @ *h*ttp://www.pas.rochester.edu/ martinhe/.